A familial missense variant in the Alzheimer's Disease gene *SORL1* impairs its maturation and endosomal sorting.

Elnaz Fazeli[1], Daniel D. Child[2], Stephanie A. Bucks[3], Miki Stovarsky[4], Gabrielle Edwards[3], Shannon E. Rose[2], Chang-En Yu[4,6], Caitlin Latimer[2], Yu Kitago[5], Thomas Bird[3,4,6], Suman Jayadev[3*], Olav M. Andersen[1*], and Jessica E. Young[2*]

***Co-corresponding authors**

[1] Department of Biomedicine, Aarhus University, Høegh-Guldbergs Gade 10, DK8000 AarhusC, Denmark

[2]Department of Laboratory Medicine and Pathology, University of Washington, Seattle Washington USA

[3]Department of Neurology, University of Washington, Seattle Washington USA

[4]Department of Medicine, Division of Medical Genetics University of Washington, Seattle Washington USA

[5]Ann Romney Center for Neurologic Diseases, Harvard Medical School and Brigham and Women's Hospital, Boston, MA 02115

[6]Geriatric Research Education and Clinical Center (GRECC), Veterans Administration Health Care System

Correspondence to: jeyoung@uw.edu, sumie@uw.edu, o.andersen@biomed.au.dk

Abstract

The *SORL1* gene has recently emerged as a strong Alzheimer's Disease (AD) risk gene. Over 500 different variants have been identified in the gene and the contribution of individual variants to AD development and progression is still largely unknown. Here, we describe a family consisting of 2 parents and 5 offspring. Both parents were affected with dementia and one had confirmed AD pathology with an age of onset >75 years. All offspring were affected with AD with ages at onset ranging from 53yrs-74yrs. DNA was available from the parent with confirmed AD and 5 offspring. We identified a coding variant, p.(Arg953Cys), in *SORL1* in 5 of 6 individuals affected by AD. Notably, variant carriers had severe AD pathology, and the *SORL1* variant segregated with

TDP-43 pathology (LATE-NC). We further characterized this variant and show that this Arginine substitution occurs at a critical position in the YWTD-domain of the *SORL1* translation product, SORL1. Functional studies further show that the p.R953C variant leads to retention of the SORL1 protein in the endoplasmic reticulum which leads to decreased maturation and shedding of the receptor and prevents its normal endosomal trafficking. Together, our analysis suggests that p.R953C is a pathogenic variant of *SORL1* and sheds light on mechanisms of how missense *SORL1* variants may lead to AD.

Running Title: Pathogenic *SORL1* variant impairs sorting

Keywords: *SORL1*; Alzheimer's disease; YWTD-domain; pathogenic variant; TDP-43

Introduction

Alzheimer Disease (AD) is the most common cause of dementia worldwide. The etiology of AD remains elusive, slowing development of disease modifying therapies. Pathogenic variants in *PSEN1*, *PSEN2* and *APP* are associated with autosomal dominantly inherited early-onset AD (ADAD), although those families are rare and make up only a very small fraction of all AD. Nevertheless, knowledge gained from studying ADAD has been valuable to our understanding of the clinical, pathological and mechanistic features of AD more broadly. Late onset AD also has a genetic component and is known to be highly heritable, estimated at 60-80%[33] and heritability can vary with age[9]. Genome wide association studies (GWAS) as well as genome and exome sequencing studies have revealed the complexity of biological processes contributing to AD risk and progression[70]. Given that families with AD likely harbor at least one AD genetic risk factor, they can provide important insight into genetic risk and disease pathogenesis.

The Sortilin-like receptor, *SORL1,* (protein: SORL1/SORLA) was originally identified as a member of the LDL receptor family, and the SORL1 protein is now classified as one of five mammalian sorting receptors called VPS10p receptors[31, 32, 72-74]. SORL1 functions as an endosomal receptor to assist cargo sorting out of the endosome to either the cell surface via the recycling pathway or to the trans-Golgi network (TGN) via the retrograde pathway[21, 24, 34, 51, 65]. For sorting of AD-related cargo, including Amyloid-β peptide (Aβ) and APP, SORL1 directly interacts with the multi-sorting complex retromer, itself highly implicated in endo-lysosomal health and neurodegeneration[18, 22, 57].

62 Through both candidate gene studies and GWAS, *SORL1* was found to be a strong genetic risk
63 factor for AD[42, 43, 58, 59]. Exome-sequencing studies have shown that rare loss-of-function
64 S*ORL1* alleles, leading to haploinsufficiency, have been associated with highly penetrant AD[25,
65 26, 55, 56, 71], although the full breadth and contribution of *SORL1* variants in AD is not fully
66 defined. A large number (>500) of *SORL1* variants have been identified in patient populations
67 with AD, but with variable levels of evidence for pathogenicity. Recently, two missense variants
68 have been associated with autosomal dominant AD: p.(Asp1545Val) (Bjarnadottir et al.,
69 Manuscript in preparation) and p.(Tyr1816Cys)[35]. In case of the p.(Tyr1816Cys) we showed
70 how this mutation has only minor impact on the intracellular localization per se, but strongly
71 decreased receptor dimerization in endosomes and retromer-dependent recycling to the cell
72 surface[35]. Reported *SORL1* variants span the length of the gene and functional domains, and
73 how different pathogenic variants impair the overall functions of SORL1 as an endosomal sorting
74 receptor is not yet clear. It has been suggested that SORL1 maturation, which is a distinct change
75 in some of the *N*-glycans attached to the luminal SORL1 domain[14], is decreased for some *SORL1*
76 missense variants[50, 60]. Defining the biochemical consequences of pathogenic *SORL1* missense
77 variants can shed light on mechanisms of disease involving SORL1 and other components of the
78 endo-lysosomal network (ELN).
79
80 We present here a family with early and late onset AD in two generations. Genetic testing
81 confirmed a novel *SORL1* variant, c.2857C>T p.Arg953Cys (R953C; NM_003105.5) which
82 affects a residue in one of the repeats in the YWTD-domain, in 6 out of 7 affected individuals
83 tested. Neuropathological studies demonstrated severe AD pathology, including cerebellar
84 amyloid plaques, cortical neurofibrillary tangles, and TDP-43 deposition despite a young age of
85 onset in most carriers of the *SORL1* R953C variant. One individual, I-2, was affected with AD but
86 did not carry the SORL1 variant and did not show TDP-43 deposition. To further characterize this
87 genetic variant, we turned to a previously described disease-mutation domain-mapping approach
88 that relies on identified pathogenic variants in homologous proteins including members of the
89 LDLR family[8], to predict pathogenicity based on the domain position at which the variant occurs
90 in SORL1. We next generated a plasmid containing the p.R953C variant and transfected it into
91 HEK293 and N2a cells. Our *in vitro* studies suggest reduced SORL1 maturation and impaired
92 endosomal localization, confirming a functional consequence of the missense variant. The

influence of the variant on SORL1 cellular localization may lead to impairment of endosomal sorting and have pathogenic effects. This study adds to the growing body of literature supporting a role for *SORL1* variants that may contribute to the missing AD heritability.

Methods

Study Participants

The family was ascertained by the University of Washington Alzheimer Disease Research Center. The study was approved by the UW Institutional Review Board (IRB) and all participants provided written consents.

Genetic Studies

Genetic analysis was performed by the Northwest Clinical Genomics Laboratory (NCGL), a CLIA certified laboratory at the University of Washington. Samples underwent next-generation exome sequencing and analysis. Libraries were constructed according to the NCGL protocol. The KAPA Hyper Prep DNA library kit (KAPA Biosystems, Wilmington, MA, USA) was used to prepare the libraries, which were subsequently enriched using an in-house, optimized xGen Exome Research Panel v1.0 (Integrated DNA Technologies, Coralville, IA, USA). Paired-end sequencing of the exome-enriched libraries was performed on a HiSeq 4000 instrument (Illumina, San Diego, CA, USA). Greater than 99% of the coding regions and canonical splice sites were sequenced to a read coverage of at least 20X or greater. The average mean depth of coverage was 144 reads. Resulting sequences were aligned to the human genome reference (hg19) using the Burrows-Wheeler Aligner (BWA)[46]. Variants were identified using the Genome Analysis Toolkit (GATK)[19, 49]and were annotated using the SnpEff annotation tool[15] in combination with various population databases and variant impact scoring tools. Individual II-5 was initially screened with a 39-gene dementia panel which included: *APP*, *ARSA, APOE, ATP13A2, CHCHD10, CHMP2B, CSF1R, DNMT1, EIF2B1, EIF2B2, EIF2B3, EIF2B4, EIF2B5, FUS, GALC, GRN, HEXA, ITM2B, LMNB1, MAPT, NOTCH3, NPC1, NPC2, OPA1, PDGFB, PDGFRB, PLP1, PRNP, PSEN1, PSEN2, SLC20A2, SLC25A12, SORL1, TARDBP, TBK1, TBP, TREM2, TYROBP, VCP* which identified the *SORL1* p.R953C variant. Whole exome sequencing was then performed on II-1, II-2, II-4 and II-5 to evaluate for any other candidate variants and to investigate which variants segregated with the phenotype. Shared variants were filtered based on population data and variants

124 with an allele frequency greater than 0.001 in ExAC were excluded from further analysis. Variants
125 were manually evaluated through literature searches in PubMed. II-1, II-2, II-4 were also found
126 to carry the *SORL1* p.R953C variant via exome sequencing. No other variants associated with
127 dementing disorders were identified. II-3 was later found to carry the variant using Sanger
128 sequencing.
129
130 *APOE genotyping:*
131 APOE genotyping was performed as previously published[44]. Briefly, genomic DNA was
132 amplified in a 9700 Gene Amp PCR System (Applied Biosystems) using primers that amplify
133 *APOE* gene's exon 4. This PCR amplicon includes both the codon 112 (ε2/ε3 vs. ε4) and codon
134 158 (ε2 vs. ε3/ε4) polymorphic sites.
135 *Taqman assay:* SNPs rs429358 (ε2/ε3 vs. ε4) and rs7412 (ε2 vs. ε3/ε4) were genotyped using
136 assay C_3084793_20 and assay C_904973_10 (Thermo Fisher), respectively. All reactions were
137 carried out in a 9700 Gene Amp PCR System with a profile of 50°C for 5 minutes; 95°C for 5
138 minutes; 50 cycles of 95°C for 15 seconds, and 60°C for 1 minute.
139 *Sanger sequencing:* The PCR reaction/amplicon (1 µl) was used in BigDye sequencing reaction
140 (Thermo Fisher) with a final volume of 10 µl. All reactions were carried out in a 9700 Gene Amp
141 PCR System with a profile of 94°C for 1 minute; 35 cycles of 94°C for 30 seconds, 55°C for 10
142 seconds, and 60°C for 4 minutes; and a final extension of 60°C for 5 minutes. The PCR generated
143 sequencing products were further purified using EDTA/ethanol precipitation and then subjected to
144 DNA sequencing run using SeqStudio (Thermo Fisher). The sequencing data (electropherograms)
145 were transferred and uploaded onto the Sequencher program (Genecodes) for sequence alignment.
146 Primer sequences:
147 APOE_Ex4_F: 5' TCGGAACTGGAGGAACAACT 3'
148 APOE_Ex4_R: 5' GCTCGAACCAGCTCTTGAGG 3'
149
150 *SORL1 genotyping*
151 *SORL1* variant genotyping was performed on I-2, II-2, II-3, and III-6. Genomic DNA was
152 amplified with Phusion Flash (Thermo Fisher) on a C1000 Touch Thermo cycler (BioRad) using
153 primers that amplify exon 20 in *SORL1*. Cycle conditions: 98°C for 10s; 98°C for 1s, 65°C for 5s,
154 72°C for 10s X25 cycles; 72°C for 1 min. Cleaned PCR reactions were sent for Sanger sequencing

155 using GeneWiz (Azenta Life Sciences). Sequences were examined manually using 4 Peaks
156 software.
157 Primer sequences:
158 *SORL1* F: 5' GCCTGGGATTTATCGGAGCA 3'
159
160 *SORL1* R: 5' TGGCATCCCTCCATAGGCT 3'
161
162 *Neuropathology*
163 Consent for autopsy was obtained from the donor or from the legal next of kin, according to the
164 protocols approved by the UW Institutional Review Board. At the time of autopsy, the brain was
165 removed in the usual fashion. For patients I-2, II-2, II-3 and II-4, the left halves were coronally
166 sectioned and samples were frozen for possible biochemical studies and the right halves were fixed
167 in formalin. For patients II-1 and II-5, the entire brain was fixed in formalin. After fixation, the
168 cerebrum was sectioned coronally, the brainstem was sectioned axially, and the cerebellum was
169 sectioned sagittally.
170
171 Representative sections for histology were selected and evaluated according to National Institute
172 of Aging-Alzheimer's Association (NIA-AA) guidelines[52]. A microtome was used to cut 4 µm-
173 thick tissue sections from formalin-fixed, paraffin-embedded tissue blocks. Hematoxylin and eosin
174 (H&E), Luxol fast blue (LFB), and Bielschowsky silver-stained slides were prepared. Using
175 previously optimized conditions, immunohistochemistry was performed using a Leica Bond III
176 Fully Automated IHC and ISH Staining System (Leica Biosystems, Wetzlar, Germany). The
177 sections were immunostained with mouse monoclonal antibody against paired helical filament tau
178 (AT8, 1:1,000 dilution) (Pierce Technology, Waltham, MA), mouse monoclonal against β-
179 amyloid (6E10, 1:5,000) (Covance, Princeton, NJ), rat monoclonal against phosphorylated TDP-
180 43 (ser409/ser410, 1:1,000) (Millipore, Burlington, MA), and mouse monoclonal against α-
181 synuclein (LB509, 1:500) (Invitrogen, Carlsbad, CA). Appropriate positive and negative controls
182 were included with each antibody and each run.
183
184 *Site-directed Mutagenesis*
185 The R953C variant was inserted in *SORL1* pcDNA3.1 and *SORL1*-GFP pcDNA3.1 using site
186 directed mutagenesis kit (QuikChange #200521) according to manufacturers' instruction with the

187 following pair of primers: 5- gga tca cgt tca gtg gcc agc agt gct ctg tca ttc tgg aca acc tcc-3 and 5-
188 gga ggt tgt cca gaa tga cag agc act gct ggc cac tga acg tga tcc-3.
189
190 *Cell transfection and western blotting*
191 Approximately $5x10^5$ HEK293 and N2a cells were seeded on 6-well plates and transiently
192 transfected with expression constructs for *SORL1*-WT or *SORL1*-R953C, using Fugene 6
193 Transfection Reagent kit (Promega) according to manufacturers' instructions. 48 hours post
194 transfection, cell medium was changed to serum free conditional medium and after 48 hours, cells
195 and media were harvested. Cells were lysed using lysis buffer (Tris 20mM, EDTA 10mM, TritonX
196 1%, NP40 1%). Media samples (30ml) and lysate samples(20ug) were mixed with NuPAGE LDS
197 sample buffer (Invitrogen, #2463558) supplemented with β-Mercaptoethanol (Sigma) and
198 separated on SDS-PAGE using 4–12% NuPAGE Bis-Tris gels (Thermo). Proteins were then
199 transferred to nitrocellulose membranes (Thermo) and incubated for 1h at room temperature in
200 Blocking buffer (Tris-Base 0.25M, NaCl 2.5M, skimmed milk powder 2%, tween-20 2%). Next,
201 membranes were incubated overnight at 4°C with LR11 antibody 1:1,000 (BDBiosciences #
202 612633) to detect SORL1 and Beta actin 1:2,000 (Sigma #A5441) as loading control, followed by
203 three washes for 5 minutes in washing buffer ($CaCl_2$ 0.2 mM, $MgCl_2$ 0.1 mM, HEPES 1 mM,
204 NaCl 14 mM, skimmed milk powder 0.2%, Tween 20 0.05%) and 1 hour incubation with HRP-
205 conjugated secondary antibody (1:1,500, Dako, #P0260) for 1 hour at room temperature.
206 Membranes were washed 5 times for 5 minutes, incubated with FEMTO detection reagent
207 (Thermo #34095) and visualized by iBright1500 scanner. Quantification was performed by
208 densitometric analysis in ImageJ and data were plotted in Graphpad Prism 9.5.0.
209
210 *Flow cytometry*
211 Cell surface and total receptor level were analyzed by flow cytometry in live, transfected HEK293
212 and N2a cells. Briefly, HEK293 and N2a cells were transiently transfected with either *SORL1*-
213 GFP-WT or *SORL1*-GFP-R953C plasmids. Twenty-four hours after transfection, cells were
214 collected by trypsinization, pelleted, and resuspended in phosphate-buffered saline (PBS pH 7.4).
215 After 15min incubation in blocking buffer (PBS pH 7.4 ,0.5% BSA), cells were immunostained at
216 4°C with rabbit anti-soluble-SORL1 primary antibody followed by washing two times with PBS
217 pH 7.4 and 30min incubation with Alexa-flour 647 secondary antibody in the absence of detergent

218 followed by 3 times washing and finally resuspension in FACS buffer (PBS pH 7.4, 2% FBS, 1%
219 Glucose). Cells were analyzed by NovoCyte 3000 flow cytometer equipped with three lasers and
220 13 fluorescence detectors (Agilent, Santa Clara, CA). GFP and Alexa Flour 647 fluorophores were
221 excited by the 488 and 640 nm lasers, respectively. Results were analyzed using FlowJo™ v10.8.1
222 Software (BD Life Sciences).
223
224 *Immunocytochemistry and Confocal Microscopy*
225 Approximately $5x10^4$ HEK293 cells were seeded on poly-L-lysine coated glass coverslips and
226 transfected with expression constructs for *SORL1*-WT or *SORL1*-R953C using Fugene 6
227 Transfection Reagent kit (Promega). 24h post-transfection, cells were fixed with PFA 4% for 10
228 minutes at room temperature, followed by a wash in PBS pH 7.4. Coverslips were washed twice
229 in PBS with 0.1% Triton-X 100 (for intracellular staining) or only PBS (for membrane staining)
230 and later blocked for 30 minutes at room temperature in blocking buffer (PBS, FBS 10%). Cells
231 were then incubated overnight at 4°C with pAb_5387 (a polyclonal rabbit serum generated for the
232 entire SORL1 ectodomain[31]) antibody alone or with an antibody against markers specific for
233 each intracellular compartment (EEA1 for early endosomes, TFR for recycling endosomes, and
234 Calnexin for ER). Next, cells were washed in PBS with or without Triton-X 0.1 % and incubated
235 in Alexa Flour secondary antibodies (Invitrogen, 1:500) for 1 hour at room temperature. After
236 washing once in PBS, cells were stained with Höechst (Abcam, 1:50,000) for 10 minutes at room
237 temperature. The coverslips were then mounted on glass slides using DAKO fluorescence
238 mounting medium (Agilent) and were imaged using Zeiss LSM800 confocal microscope.
239 Colocalization was quantified using the JACOP plugin in ImageJ software and presented as
240 Mander's correlation coefficient. Graphing and statistical analysis of the data were performed with
241 GraphPad Prism 9.5.0. Antibodies used were as follows: rabbit polyclonal anti-SORL1
242 (pAb_5387; Aarhus University) 1:300, mouse monoclonal anti-SORL1 (mAb_AG4; Aarhus
243 University) 1:100, anti EEA1(#610457 BDBiosciences) 1:100, anti TFR 1:100(# A-11130
244 Invitrogen), anti-Calnexin (1:100) (#610523 BDBiosciences).
245
246 *Statistical analysis.*
247 The data are represented as the mean ± s.d. The 'n' numbers represent the number of biological
248 replicates in each experiment, while for imaging studies 'n' represents the total number of cells

analyzed. Data was analyzed using parametric two-tailed paired (WB analysis and flow cytometry) or unpaired (immunostaining) t-tests. A P-value of less than 0.05 is considered statistically significant. All statistical analysis was completed using GraphPad Prism 9.5.0 software.

Data Availability

The authors confirm that the data supporting the findings of this study are available within the article and/or its supplementary material or available from a corresponding author upon reasonable request.

Results

Clinical Description

Three generations (**Figure 1**) of the study family are presented here. Clinical features are reported in **Table 1**. Both parents (I-1 and I-2) developed late onset dementia and I-1 also demonstrated parkinsonism and aggressive behavior. Of the 5 individuals in the II generation sibship, 4 were clinically diagnosed with AD, with a range of age of onset from 51 years to 73 years. II-3 was reported to carry a clinical diagnosis of dementia prior to death and had age of onset 74 yrs. II-4 and II-5, identical twins, developed early onset AD at age 57 years and 51 years, respectively. II-5 developed aphasia and apraxia in addition to memory loss. III-6, daughter of II-2, developed progressive spasticity at age 44. She has also developed evidence of executive dysfunction determined by neuropsychiatric evaluation at age 45 and again on repeat testing at age 46 without progression. She has not shown any lower motor neuron findings or any other neurological signs. MRI brain did not show atrophy or other abnormality (data not shown).

Neuropathology

Individuals I-2, II-1, II-2, II-3, II-4, and II-5 were evaluated at autopsy, and findings are summarized in **Table 2**. Brain weight in all cases except II-1 was below the 10th percentile for age and sex[10]. Atherosclerosis was present in all cases, with plaques extending beyond the first branch point of at least one cerebral artery (defined here as moderate); in case II-4, atherosclerotic plaques were also visible on the external surface and thus graded as severe. No other abnormalities were observed grossly in any case.

Histopathology

All autopsy cases were evaluated by the standard NIA-AA protocol[30, 52]. β-amyloid plaques progressed to the midbrain in cases I-2 and II-1 (Thal phase 4 of 5), and extended to the cerebellum in cases II-2, II-3, II-4, and II-5 (Thal phase 5 of 5, **Figure 2a**). Tau tangles were present within the calcarine cortex/primary visual cortex in all cases (Braak and Braak stage VI of VI, **Figure 2b**). Cortical neuritic plaque density in all cases was frequent by Consortium to Establish a Registry for Alzheimer's Disease (CERAD) criteria (**Figure 2c**). The features in each case meet criteria for high Alzheimer's disease neuropathologic change (ADNC) by NIA-AA guidelines[52]. Additionally, all generation II cases had TDP-43 inclusions in the amygdala and hippocampus,

290 consistent with limbic-predominant age-related TDP-43 encephalopathy neuropathologic change
291 (LATE-NC) stage 1 or 2 out of 3[53] (**Figure 2d**); TDP-43 inclusions were not seen in case I-2
292 (*SORL1* variant negative). Hippocampal sclerosis was also seen in cases II-2 and II-4. Varying
293 stages of Lewy body disease (LBD) were also identified, with diffuse (neocortical) LBD diagnosed
294 in II-1, limbic (transitional) LBD in II-2, and brainstem-predominant LBD in II-4 (**Figure 2e).** We
295 present neuropathological findings of all subjects that underwent brain autopsy in **Figure 3.**
296
297 *Genetic Findings*
298 Due to early onset and family history of AD, subject II-5 underwent *PSEN1* and *APP* research
299 genetic testing, which was negative in both genes. Years after the subject's passing, his genetic
300 material was included in an early onset AD cohort evaluated by an exome panel of 39
301 neurodegeneration genes. II-5 was found to carry a *SORL1* missense variant: NM_003105.5
302 c.2857C>T p.Arg953Cys (R953C). The reported allele frequency of this variant in gnomAD for
303 those of European (non-Finnish) ancestry is 1/113646. It has not been reported in other populations
304 assessed. In silico predictions varied; Polyphen: probably damaging, SIFT: tolerated, REVEL:
305 0.805, CADD v1.3: 25.4, PrimateAI: 0.633. No other pathogenic or likely pathogenic variants
306 were identified in the other 38 genes on the neurodegeneration panel. Next, we screened II-1, II-
307 2, II-4, and II-5 by whole exome sequencing, which revealed that all four subjects carry the *SORL1*
308 R953C variant and no other pathogenic variants known to be associated with dementia were
309 identified. We re-confirmed the presence of the *SORL1* R953C in II-2 variant using Sanger
310 sequencing. II-3 passed away during preparation of this manuscript. We performed Sanger
311 sequencing and confirmed the presence of the *SORL1* R953C variant in II-3. Using Sanger
312 sequencing, we found that I-2 did not carry the *SORL1* variant, and no DNA samples were
313 available from I-1. III-6 was found to carry the *SORL1* variant using Sanger sequencing of dermal
314 fibroblasts. All Sanger sequencing results are presented in **Supplemental Figure 1**. C9orf72 gene
315 expansion testing was negative in generation II and III-6. I-2, all individuals in the II generation
316 and III-6 have an APOE ε3/ε3 genotype.
317
318 *Variant characterization*
319 The arginine residue Arg953 is located at blade position 38 of the YWTD-domain repeated
320 sequence, located within the fifth of six repeats that build the 6-bladed β-propeller domain of

321 SORL1 (**Figure 4a**). We previously undertook a detailed disease-mutation domain-mapping
322 approach to identify the most pathogenic sequence positions for the SORL1 domains and their risk
323 for developing AD[8]. From this analysis, YWTD-domain sequence position 38 was identified as
324 a high-risk site when arginine substitution occurs, and we identified variant p.Arg953His,
325 (p.R953H) in three early-onset AD patients corresponding to the same SORL1 amino acid.
326 However, the p.R953C variant was not identified in this large exome-sequencing study[25]. From
327 previous disease mapping work[8], we identified 5 pathogenic variants in homologous proteins
328 corresponding to substitution of an arginine at the YWTD-domain sequence position 38,
329 summarized in **Table 3**. We report variant classification by VarSome, a search engine that
330 aggregates databases, including ClinVar, and annotates pathogenicity of variants using the
331 ACMG/AMP guidelines[41].
332 Familial hypercholesterolemia (FH) is an autosomal dominant disorder with a prevalence of
333 approximately 1 in 500 and most frequently caused by mutations in the gene for the low-density
334 lipoprotein receptor (LDLR). The variant p.R595W^{LDLR} has been identified in patients with FH
335 family history in cohorts from Belgium[20] and Taiwan[13] and considered an autosomal
336 dominant variant.
337 Variants in another member of the LDLR gene family, LRP5, has been associated with a number
338 of monogenic diseases, and different variants are often the cause of different clinical disorders.
339 The p.R1188W^{LRP5} has been identified to segregate in a 40-member Dutch family with three
340 generations of early- and late-onset cystogenesis inherited in an autosomal dominant fashion with
341 Polycystic Liver Disease (PCLD). Cell-based studies to assess receptor activity confirmed
342 significantly decreased activity of the mutated receptor compared to wild-type LRP5[16].
343 Osteoporosis-Pseudoglioma Syndrome (OPPG) is an autosomal recessive disorder and is caused
344 by homozygous pathogenic variants in LRP5, due to the receptor function as a key regulator of
345 bone metabolism through the Wnt signaling pathway. The biallelic presence of the pathogenic
346 variant p.R494Q^{LRP5} has been identified as the cause of OPPG in families with homozygous
347 carriers of the mutation[1, 3, 23]. Moreover, the p.R494W^{LRP5} that affects the same amino acid of
348 LRP5 was identified as a potential pathogenic variant in a patient with Familial Exudative
349 Vitreoretinopathy (FEVR), adding further support to the critical role of this amino acid to produce
350 functional LRP5[47].
351

352 The variant p.R752G^{LRP5} was also identified as the cause of disease in a compound homozygous
353 carrier for the FEVR autosomal recessive disorder [36]. Another variant that affects the same
354 amino acid in LRP5; p.R752W^{LRP5} has been reported to associate with low bone mineral density
355 in a female heterozygous carrier, and in combination with another pathogenic LRP5 variant
356 (p.W79R that affects a YWTD-motif residue) in her son causes a severe case of compound
357 heterozygous OPPG[4]. Moreover, the p.R752W^{LRP5} was identified as a potential pathogenic
358 variant in a patient with FEVR when it was identified in a compound heterozygous carrier together
359 with the pathogenic p.C1305Y variants in LRP5[27]. These studies add further support to the
360 critical role of the arginine amino acid at domain position 38 to produce functional LRP5. A
361 variant, p.R632H^{LRP4}, affects the homologous receptor LRP4. This variant is causal for
362 sclerosteosis when present as heterozygous compound mutation together with another pathogenic
363 variant in LRP4 (p.R1170Q). Cell based assays confirmed how both of these mutations in LRP4
364 reduced receptor activity, providing support of the important function of the arginine also within
365 the YWTD-domain of LRP4[29]. We summarize these findings and literature in **Table 3**.
366
367 We recently prepared a three-dimensional model of the SORL1 ectodomain including its YWTD-
368 domain using the AlphaFold2 algorithm[34]. Here, we used this model to investigate the
369 functional role of the arginine side chain (**Figure 4b, d**). From this model it is observed that the
370 positively charged amino group makes ionic contacts with the side chain of the glutamic acid
371 residue at blade-sequence position 28 (E944 of SORL1) serving to position the long arginine side
372 chain in place to make further hydrogen bonds to two backbone carbonyls in the preceding loop
373 between blades (**Figure 4d**), thereby strongly contributing to the folding and the stability of the
374 entire six-bladed β-propeller domain. Interestingly, in four of the five blade-sequences containing
375 the identified disease variants, a glutamic acid is similarly located at blade-sequence position 28
376 (**Figure 4c**).
377
378 Inspection of a larger alignment of YWTD-repeat sequences revealed that for most blade-
379 sequences, a similar pattern is observed: when an arginine occupies blade-sequence at position 38,
380 then a glutamate resides at blade-sequence position 28[8], suggesting this pair of residues may
381 generally be important for the folding of YWTD-domains.
382

383 The crystal structures of the YWTD-domains have previously been solved for LDLR[61] and
384 LPR4[75] including R595^{LDLR} and R632^{LRP4}, the homologous residues for R953^{SORL1},
385 respectively. The structure of LRP5 has not been determined, but as the crystal structure of the
386 highly homologous LRP6 has been solved[2, 11, 12], it allowed us to use these YWTD-domain
387 structures to gain insight in the functional role of the arginine side chain for the arginines at blade-
388 sequence position 38 as well as for the LRP5 residues (R494^{LRP5}/R481^{LRP6}; R752^{LRP5}/R739^{LRP6};
389 R1188^{LRP5}/R1178^{LRP6}) (**Figure 4e**). Indeed, we found that the arginine side chains in each of the
390 domains are binding backbone carbonyls in the n-1 linker, and for 4 of the 5 structures a salt bridge
391 to a glutamic acid (at domain position 28) assist in keeping the arginine properly positioned to
392 make the main chain interactions to the n-1 linker residue (**Figure 4e**). This supports a disease
393 mechanism where substitution of the arginine may lead to domain misfolding and destabilization
394 in general, and importantly also for R953 of SORL1.
395
396 *R953C disrupts SORL1 maturation and ectodomain shedding from the cell surface*
397 SORL1 protein is synthesized in the ER and goes through a complex cellular process of maturation
398 during trafficking in the ER and out of the Golgi into the ELN compartments and to the cell surface.
399 The mature SORL1 isoform has complex-type *N*-glycosylations, and we previously showed only
400 mature *N*-glycosylated SORL1 is shed from the cell surface to produce a fragment called soluble
401 SORL1 (sSORL1)[14], and therefore a decrease in sSORL1 is often a direct measure of the
402 maturation process being decreased for folding-deficient SORL1 mutant protein. Mature SORL1
403 migrates more slowly by SDS-PAGE, thus mature and immature isoforms of cellular SORL1 can
404 be clearly distinguished[63] (**Figure 5a**).
405 To test whether the p.R953C variant affects SORL1 maturation and shedding, we transfected
406 HEK293 and N2a cells with either the SORL1-WT or a SORL1-R953C construct. We performed
407 Western blot analysis to determine the ratio of the mature to immature forms of the protein. We
408 observed significantly decreased levels of mature SORL1 in HEK293 cells transfected with the
409 R953C variant (**Figure 5a**). We next measured the level of sSORL1 in the culture medium of
410 HEK293 and N2a cells, transiently transfected with expression constructs for SORL1-WT or
411 SORL1-R953C. Compared to cells transfected with WT construct, we observed ~ 80% reduction
412 in the sSORL1 level in the media from both the tested cell types transfected with the R953C
413 construct (**Figure 5a, b**)

414 *R953C reduces cell surface expression of SORL1*

415 Because we observed a significant decrease in the shedding of SORL1-R953C, we tested whether
416 the cell surface level of SORL1 could also be affected by this variant. We transiently transfected
417 HEK293 cells with either SORL1-WT or SORL1-R953C and first analyzed cell surface levels of
418 SORL1 using immunocytochemistry on unpermeabilized cells, which keeps the membrane intact
419 to allow visualization of SORL1 protein solely located at the cell membrane. Using confocal
420 microscopy, we observed considerably fewer cells expressing SORL1 at the cell surface in cells
421 transfected with SORL1-R953C compared to SORL1-WT (**Figure 6a**). To quantitatively evaluate
422 cell surface expression of SORL1-R953C relative to the total expression of the receptor in each
423 individual cell, we used flow cytometry. We inserted the R953C variant into a C-terminally GFP
424 tagged SORL1 construct, allowing for the detection of total expression of the receptor in each
425 individual cell. We transfected both HEK293 cells and N2a cells and performed subsequent
426 immunostaining of the transfected cells with anti-sSORL1 primary antibody and an Alexa Flour
427 647 secondary antibody in the absence of detergent to detect the cell surface expression of the
428 receptor. These experiments demonstrated that more than 80% of the SORL1-R953C cells partially
429 or completely retained SORL1 expression intracellularly compared to ~10-15% of the SORL1-
430 WT cells. Results were consistent in both HEK293 and N2a cells (**Figure 6b-c**).

431

432 *R953C prevents SORL1 from entering the endosomal recycling pathway*

433 The differential cell surface localization and shedding of the R953C variant compared to WT led
434 us to next investigate for possible changes in the intracellular localization of SORL1. For these
435 experiments we transiently transfected HEK293 cells with either *SORL1*-WT or *SORL1*-R953C
436 constructs. We analyzed co-localization of WT and R953C with two well-established endosomal
437 markers, EEA1 (early endosome marker) and TFR (recycling endosome marker) and the ER
438 marker Calnexin, 24 hours post-transfection. Using confocal microscopy, we demonstrated that
439 the colocalization of R953C is strongly reduced with both endosomal markers (**Figure 7a-b**) and
440 significantly increased in the ER (**Figure 7c**). Taken together, these data suggest that the R953C
441 variant severely disrupts the normal cellular localization trafficking of SORL1 as would be
442 expected if the mutation leads to defective protein folding.

443

Discussion

SORL1 is widely recognized as a strong AD risk gene though less is known about the AD risk attributable to rare missense variants[26, 55, 62]. Here we describe a family with two generations of both early and late onset AD in which we obtained brain autopsy pathology on 6 affected family members which enabled correlating clinical phenotype, genotype and neuropathology. Here we provide clinicopathological, genetic, and functional data supporting pathogenicity of a novel rare *SORL1* missense variant, p.(Arg953Cys) (R953C). Five of the five offspring were found to have the *SORL1* variant, and their age of onset ranged from 51yrs – 74 years. Notably, all affected individuals, including the mother who was WT for *SORL1* R953C, were of APOE3/3 genotype suggesting that APOE status was not contributing to risk or age of onset. Tissue from the mother (I-2) was analyzed by Sanger sequencing and found not to harbor R953C and tissue from the father was not available to confirm whether the allele was paternally inherited. Given the range of onset it is possible that additional genetic factors inherited from either parent has influenced expression of AD in both generations. Of note one living member of the family has been genotyped and is found to carry the variant (III-6) but is younger than the range of age of onset for the family. It is unknown whether her 3-year course of spasticity is related to the *SORL1* variant or is an unrelated case of a neurologic disease.

Neuropathology examination shows the presence of severe AD pathology, including extensive plaque and neurofibrillary tangle distribution. These histologic features typically correlate with advanced clinical disease[30, 52]. There are very few studies of neuropathology on *SORL1* variant carriers. There is one report of a *SORL1* homozygous truncating variant (c.364C>T, p.R122*) that shows severe cerebral amyloid angiopathy in addition to AD neuropathology as well as a patient with a splicing variant (c.4519+5G>A) in which AD was confirmed by neuropathological studies[5]. Yet another study shows SORL1 immunoreactivity in glial cells and white matter in a family with a *SORL1* variant c.3907C>T, p. R1303C.[69].

In our study, all cases underwent an extensive neuropathology examination in accordance with the most up-to-date guidelines for AD and related dementias[52, 53]. In this way, we were able to identify the presence of LATE-NC, marked by accumulation of TDP-43[53]. Interestingly, *SORL1* R953C segregated with LATE-NC pathology in 5 out of 5 offspring and with earlier age at AD

475 onset in 3 out of 5 offspring. In fact, a recent analysis linked carrying a variant in *SORL1* with
476 LATE-NC[38]. Although LATE-NC is a common co-pathology identified in AD, the underlying
477 etiology of this TDP-43 pathology is not well understood. Age seems to be the strongest risk factor
478 and it is most frequently noticed in individuals older than 80 years[53, 54]. Similar to other age-
479 related neuropathologic changes, LATE-NC frequently co-occurs with other pathologies such as
480 AD and/or hippocampal sclerosis[6], and its presence may accelerate the cognitive decline
481 associated with these disorders[37]. It is worth acknowledging that it is possible that the co-morbid
482 pathology of LATE-NC is driving the earlier age of onset in this family. Additionally, Lewy body
483 disease (LBD) was frequently observed in *SORL1* R953C carriers (**Figure 3**). One other report in
484 the literature has associated SNPs in *SORL1* with LBD, but also implicates SNPs in *APOE* and
485 *BIN1* in this association as well[17]. While LBD limited to the amygdala is frequently observed
486 in association with advanced ADNC[30, 52], ADAD due to *PSEN1*, *PSEN2* and *APP* have been
487 associated with brainstem, limbic and diffuse LBD[45, 48] similar to what we find in this family.
488 However, it is possible SORL1 itself contributes directly to synuclein pathology. Together, these
489 co-pathologies suggest that SORL1 R953C may be mechanistically linked to multiple
490 proteinopathies, clinically manifesting as AD but also impacting TDP-43[38] and α-synuclein
491 histopathology[17]. While SORL1 and a-synuclein have not been shown to directly interact, a-
492 synuclein is internalized via clathrin-mediated endocytosis and is present in many arms of the
493 endo-lysosomal network[67]. Loss of TDP-43 function affects recycling endosomes and impairs
494 trophic signaling in neurons[64]. Therefore, while there might not be a direct interaction,
495 dysfunction of SORL1 as an endosomal receptor that facilitates endosome sorting pathways may
496 lead to more global impairments in endo-lysosomal network function that affect other proteins
497 involved in neurodegeneration.
498
499 We performed analyses to examine cellular and extracellular levels of SORL1 as well as
500 experiments to determine the localization of the R953C variant withing cells. Decreased SORL1
501 levels are known to be pathogenic as truncation variants leading to haploinsufficiency have been
502 definitively linked to AD [25, 26, 62]. Furthermore, human neuronal models of *SORL1* deficiency
503 show impairments in endosomal trafficking and recycling[28, 40, 51] as do neurons from minipigs
504 with only one functional SORL1 allele[7]. One main function of SORL1 is to sort cargo from the
505 early endosome to either the recycling pathway (cell surface) or the retrograde pathway (TGN) in

506 conjunction with the multi-protein complex retromer[22, 66]. The cellular localization of SORL1
507 and the cargo it binds depend on the specific isoform: monomer vs. dimer, mature vs. immature.
508 For protein maturation, SORL1 transits through the Golgi and the trans-Golgi network to the
509 endosome and to the cell surface. Here, we demonstrate that the R953C variant of SORL1 does
510 not undergo maturation and is not shed from the cell surface.
511
512 We have recently found that two pathogenic *SORL1* missense variants associated with ADAD are
513 located in either one of the CR-domains (Bjarnadottir et al., Manuscript in preparation) or the 3Fn-
514 domains[35] respectively, and both display significantly impaired maturation and shedding. We
515 have also previously observed that sSORL1 is significantly decreased in the CSF from several
516 carriers of other established pathogenic SORL1 variants (Andersen lab, unpublished data).
517 Furthermore, a larger screen of 70 SORL1 coding variants suggested that impaired maturation may
518 be a common dysfunction of SORL1 mutant proteins[60].
519
520 Our study suggests that SORL1 R953C likely cannot function as a normal endosomal receptor, as
521 it fails to enter the endosomal pathway. Instead, it is sequestered in the ER. When the receptor gets
522 retained in the ER, it will lead to a decrease in SORL1 activity in endosomal compartments, so a
523 direct effect of ER retention is lack-of-activity of SORL1 in the endo-lysosomal pathway.
524 However, there could also be a gain-of-toxic-activity associated with the ER retained misfolded
525 receptor that potentially could lead to neurotoxic ER-stress, which is suggested to occur with
526 certain pathogenic variants in the homologous LDLR[39, 68]. Furthermore, the ER-retained
527 SORL1 mutant protein may have additional negative impacts on total receptor activity in the
528 endosome and thus increase the pathogenicity of the variant. In this scenario, the mutated receptor
529 could dimerize (or even polymerize) with the wild-type receptor, thus sequestering additional wild-
530 type SORL1 in the ER, potentially acting via a dominant-negative mechanism in diploid cells.
531 Structural analysis indicates that this variant occurs at a critical arginine in the YWTD β-propeller
532 domain of SORL1 that appears to be necessary for the proper folding of the domain. When
533 compared against homologous domains in the LDLR receptor family, arginine substitutions at this
534 position are strongly suspected to be pathogenic.
535 Finally, we demonstrate that this variant likely impedes SORL1 from entering the endosomal
536 sorting pathway. SORL1 is an endosomal receptor for many proteins that are important for proper

537 neuronal function. We and others have shown that loss of SORL1 leads to endosomal 'traffic jams'
538 and mis-localization of neurotrophic receptors and glutamate receptor subunits[51]. Loss of
539 SORL1 in the endosomal sorting pathway will likely affect multiple aspects of neuronal health
540 and function, contributing to neurodegeneration.
541
542 Over 500 variants in *SORL1* have been identified and recent genetic studies have provided
543 evidence as to which variants may be likely pathogenic or likely benign[25]. However, with such
544 a large gene (encoding for more than 2200 amino acids), more variants are likely to be identified.
545 Functional analysis of *SORL1* variants will be an important tool to classify these variants based on
546 their cellular pathogenicity and further uncover their contribution to the development of AD.
547

Acknowledgements

The authors are grateful to the family whose participation made this work possible.

Flow cytometry was performed at the FACS Core Facility, Aarhus University, Denmark.
The authors acknowledge AU Health Bioimaging Core Facility for the use of equipment and support of the imaging facility.

The authors thank the members of the University of Washington Medicine Center for Precision Diagnostics for technical support, the Geriatric Research, Education, and Clinical Center at the VA Puget Sound Health Care System, and University of Washington's Alzheimer Disease Research Center.

We acknowledge Harald Frankowski in the Young lab for preparation of gDNA samples for SORL1 variant sequencing and all members of the Young lab for helpful discussions on this work.

Funding

O.M.A is supported by Novo Nordisk Foundation (#NNF20OC0064162), the Alzheimer's Association (ADSF-21-831378-C), the EU Joint Programme-Neurodegenerative Disease Research (JPND) Working Group SORLA-FIX under the 2019 ''Personalized Medicine'' call (funded in part by the Danish Innovation Foundation and the Velux Foundation Denmark), and the Danish Alzheimer's Research Foundation (recipient of the 2022 Basic Research Science Award).

J.E.Y is supported by NIH grants R01 AG062148, K01 AG059841; an Alzheimer's Association Research Grant 23AARG1022491; a Sponsored Research Agreement from Retromer Therapeutics and a generous gift from the Ellison Foundation (to UW).
D.D.C. is supported by the Alzheimer's Disease Training Program (ADTP): T32 AG052354-06A1
Clinical and pathological work is supported by the Alzheimer's Disease Research Center (P30 AG05136)

Competing Interests

O.M.A. is a consultant for Retromer Therapeutics and has equity. The other authors report no competing interests.

References

1 Abdel-Hamid MS, Elhossini RM, Otaify GA, Abdel-Ghafar SF, Aglan MS (2022) Osteoporosis-pseudoglioma syndrome in four new patients: identification of two novel LRP5 variants and insights on patients' management using bisphosphonates therapy. Osteoporos Int 33: 1501-1510 Doi 10.1007/s00198-022-06313-1

2 Ahn VE, Chu ML, Choi HJ, Tran D, Abo A, Weis WI (2011) Structural basis of Wnt signaling inhibition by Dickkopf binding to LRP5/6. Dev Cell 21: 862-873 Doi 10.1016/j.devcel.2011.09.003

3 Ai M, Heeger S, Bartels CF, Schelling DK, Osteoporosis-Pseudoglioma Collaborative G (2005) Clinical and molecular findings in osteoporosis-pseudoglioma syndrome. Am J Hum Genet 77: 741-753 Doi 10.1086/497706

4 Alonso N, Soares DC, E VM, Summers GD, Ralston SH, Gregson CL (2015) Atypical femoral fracture in osteoporosis pseudoglioma syndrome associated with two novel compound heterozygous mutations in LRP5. J Bone Miner Res 30: 615-620 Doi 10.1002/jbmr.2403

5 Alvarez-Mora MI, Blanco-Palmero VA, Quesada-Espinosa JF, Arteche-Lopez AR, Llamas-Velasco S, Palma Milla C, Lezana Rosales JM, Gomez-Manjon I, Hernandez-Lain A, Jimenez Almonacid Jet al (2022) Heterozygous and Homozygous Variants in SORL1 Gene in Alzheimer's Disease Patients: Clinical, Neuroimaging and Neuropathological Findings. Int J Mol Sci 23: Doi 10.3390/ijms23084230

6 Amador-Ortiz C, Lin WL, Ahmed Z, Personett D, Davies P, Duara R, Graff-Radford NR, Hutton ML, Dickson DW (2007) TDP-43 immunoreactivity in hippocampal sclerosis and Alzheimer's disease. Ann Neurol 61: 435-445 Doi 10.1002/ana.21154

7 Andersen OM, Bogh N, Landau AM, Ploen GG, Jensen AMG, Monti G, Ulhoi BP, Nyengaard JR, Jacobsen KR, Jorgensen MMet al (2022) A genetically modified minipig model for Alzheimer's disease with SORL1 haploinsufficiency. Cell Rep Med 3: 100740 Doi 10.1016/j.xcrm.2022.100740

8 Andersen OM, Monti, G, Jensen A.M.G., de Waal, M., Hulsman, M., Olsen J.G., Holstege, H. (2023) Relying on the relationship with known disease-causing variants in homologus proteins to predict pathogenicity of SORL1 variants in Alzheimer’s disease. BioRxiv doi.org/10.1101/2023.02.27.524103:

9 Baker E, Leonenko G, Schmidt KM, Hill M, Myers AJ, Shoai M, de Rojas I, Tesi N, Holstege H, van der Flier WMet al (2023) What does heritability of Alzheimer's disease represent? PLoS One 18: e0281440 Doi 10.1371/journal.pone.0281440

10 Bell MD, Long T, Roden AC, Cooper FI, Sanchez H, Trower C, Martinez C, Hooper JE, Autopsy Committee of the College of American P (2022) Updating Normal Organ Weights

619 Using a Large Current Sample Database. Arch Pathol Lab Med 146: 1486-1495 Doi
620 10.5858/arpa.2021-0287-OA
621 11 Bourhis E, Wang W, Tam C, Hwang J, Zhang Y, Spittler D, Huang OW, Gong Y, Estevez A,
622 Zilberleyb Iet al (2011) Wnt antagonists bind through a short peptide to the first beta-
623 propeller domain of LRP5/6. Structure 19: 1433-1442 Doi 10.1016/j.str.2011.07.005
624 12 Cheng Z, Biechele T, Wei Z, Morrone S, Moon RT, Wang L, Xu W (2011) Crystal structures
625 of the extracellular domain of LRP6 and its complex with DKK1. Nat Struct Mol Biol 18:
626 1204-1210 Doi 10.1038/nsmb.2139
627 13 Chiou KR, Charng MJ (2010) Detection of mutations and large rearrangements of the low-
628 density lipoprotein receptor gene in Taiwanese patients with familial
629 hypercholesterolemia. Am J Cardiol 105: 1752-1758 Doi 10.1016/j.amjcard.2010.01.356
630 14 Christensen S, Narimatsu, Y., Simoes S., Goth CK., Vaegter CB., Small SA., Clausen H.,
631 Andersen, OM. (2020) Endosomal trafficking is required for glycosylation and normal
632 maturation of the Alzheimer's-associated protein sorLA. BioRxiv: Doi
633 https://doi.org/10.1101/2020.07.12.199885
634 15 Cingolani P, Platts A, Wang le L, Coon M, Nguyen T, Wang L, Land SJ, Lu X, Ruden DM
635 (2012) A program for annotating and predicting the effects of single nucleotide
636 polymorphisms, SnpEff: SNPs in the genome of Drosophila melanogaster strain w1118;
637 iso-2; iso-3. Fly (Austin) 6: 80-92 Doi 10.4161/fly.19695
638 16 Cnossen WR, te Morsche RH, Hoischen A, Gilissen C, Chrispijn M, Venselaar H, Mehdi S,
639 Bergmann C, Veltman JA, Drenth JP (2014) Whole-exome sequencing reveals LRP5
640 mutations and canonical Wnt signaling associated with hepatic cystogenesis. Proc Natl
641 Acad Sci U S A 111: 5343-5348 Doi 10.1073/pnas.1309438111
642 17 Dai DL, Tropea TF, Robinson JL, Suh E, Hurtig H, Weintraub D, Van Deerlin V, Lee EB,
643 Trojanowski JQ, Chen-Plotkin AS (2020) ADNC-RS, a clinical-genetic risk score, predicts
644 Alzheimer's pathology in autopsy-confirmed Parkinson's disease and Dementia with Lewy
645 bodies. Acta Neuropathol 140: 449-461 Doi 10.1007/s00401-020-02199-7
646 18 Daly JL, Danson CM, Lewis PA, Zhao L, Riccardo S, Di Filippo L, Cacchiarelli D, Lee D, Cross
647 SJ, Heesom KJet al (2023) Multi-omic approach characterises the neuroprotective role of
648 retromer in regulating lysosomal health. Nat Commun 14: 3086 Doi 10.1038/s41467-023-
649 38719-8
650 19 DePristo MA, Banks E, Poplin R, Garimella KV, Maguire JR, Hartl C, Philippakis AA, del
651 Angel G, Rivas MA, Hanna Met al (2011) A framework for variation discovery and
652 genotyping using next-generation DNA sequencing data. Nat Genet 43: 491-498 Doi
653 10.1038/ng.806
654 20 Descamps OS, Gilbeau JP, Leysen X, Van Leuven F, Heller FR (2001) Impact of genetic
655 defects on atherosclerosis in patients suspected of familial hypercholesterolaemia. Eur J
656 Clin Invest 31: 958-965 Doi 10.1046/j.1365-2362.2001.00915.x
657 21 Dumanis SB, Burgert T, Caglayan S, Fuchtbauer A, Fuchtbauer EM, Schmidt V, Willnow TE
658 (2015) Distinct Functions for Anterograde and Retrograde Sorting of SORLA in
659 Amyloidogenic Processes in the Brain. J Neurosci 35: 12703-12713 Doi
660 10.1523/JNEUROSCI.0427-15.2015
661 22 Fjorback AW, Seaman M, Gustafsen C, Mehmedbasic A, Gokool S, Wu C, Militz D, Schmidt
662 V, Madsen P, Nyengaard JRet al (2012) Retromer binds the FANSHY sorting motif in SorLA

663 to regulate amyloid precursor protein sorting and processing. J Neurosci 32: 1467-1480
664 Doi 10.1523/JNEUROSCI.2272-11.2012
665 23 Gong Y, Slee RB, Fukai N, Rawadi G, Roman-Roman S, Reginato AM, Wang H, Cundy T,
666 Glorieux FH, Lev Det al (2001) LDL receptor-related protein 5 (LRP5) affects bone accrual
667 and eye development. Cell 107: 513-523 Doi 10.1016/s0092-8674(01)00571-2
668 24 Herskowitz JH, Offe K, Deshpande A, Kahn RA, Levey AI, Lah JJ (2012) GGA1-mediated
669 endocytic traffic of LR11/SorLA alters APP intracellular distribution and amyloid-beta
670 production. Mol Biol Cell 23: 2645-2657 Doi 10.1091/mbc.E12-01-0014
671 25 Holstege H, Hulsman M, Charbonnier C, Grenier-Boley B, Quenez O, Grozeva D, van Rooij
672 JGJ, Sims R, Ahmad S, Amin Net al (2022) Exome sequencing identifies rare damaging
673 variants in ATP8B4 and ABCA1 as risk factors for Alzheimer's disease. Nat Genet 54: 1786-
674 1794 Doi 10.1038/s41588-022-01208-7
675 26 Holstege H, van der Lee SJ, Hulsman M, Wong TH, van Rooij JG, Weiss M, Louwersheimer
676 E, Wolters FJ, Amin N, Uitterlinden AGet al (2017) Characterization of pathogenic SORL1
677 genetic variants for association with Alzheimer's disease: a clinical interpretation strategy.
678 Eur J Hum Genet 25: 973-981 Doi 10.1038/ejhg.2017.87
679 27 Hull S, Arno G, Ostergaard P, Pontikos N, Robson AG, Webster AR, Hogg CR, Wright GA,
680 Henderson RHH, Martin CAet al (2019) Clinical and Molecular Characterization of Familial
681 Exudative Vitreoretinopathy Associated With Microcephaly. Am J Ophthalmol 207: 87-98
682 Doi 10.1016/j.ajo.2019.05.001
683 28 Hung C, Tuck E, Stubbs V, van der Lee SJ, Aalfs C, van Spaendonk R, Scheltens P, Hardy J,
684 Holstege H, Livesey FJ (2021) SORL1 deficiency in human excitatory neurons causes APP-
685 dependent defects in the endolysosome-autophagy network. Cell Rep 35: 109259 Doi
686 10.1016/j.celrep.2021.109259
687 29 Huybrechts Y, Boudin E, Hendrickx G, Steenackers E, Hamdy N, Mortier G, Martinez Diaz-
688 Guerra G, Bracamonte MS, Appelman-Dijkstra NM, Van Hul W (2021) Identification of
689 Compound Heterozygous Variants in LRP4 Demonstrates That a Pathogenic Variant
690 outside the Third beta-Propeller Domain Can Cause Sclerosteosis. Genes (Basel) 13: Doi
691 10.3390/genes13010080
692 30 Hyman BT, Phelps CH, Beach TG, Bigio EH, Cairns NJ, Carrillo MC, Dickson DW, Duyckaerts
693 C, Frosch MP, Masliah Eet al (2012) National Institute on Aging-Alzheimer's Association
694 guidelines for the neuropathologic assessment of Alzheimer's disease. Alzheimers
695 Dement 8: 1-13 Doi 10.1016/j.jalz.2011.10.007
696 31 Jacobsen L, Madsen P, Jacobsen C, Nielsen MS, Gliemann J, Petersen CM (2001) Activation
697 and functional characterization of the mosaic receptor SorLA/LR11. J Biol Chem 276:
698 22788-22796 Doi 10.1074/jbc.M100857200
699 32 Jacobsen L, Madsen P, Moestrup SK, Lund AH, Tommerup N, Nykjaer A, Sottrup-Jensen L,
700 Gliemann J, Petersen CM (1996) Molecular characterization of a novel human hybrid-type
701 receptor that binds the alpha2-macroglobulin receptor-associated protein. J Biol Chem
702 271: 31379-31383 Doi 10.1074/jbc.271.49.31379
703 33 Jayadev S (2022) Genetics of Alzheimer Disease. Continuum (Minneap Minn) 28: 852-871
704 Doi 10.1212/CON.0000000000001125
705 34 Jensen AMG, Kitago Y, Fazeli E, Vaegter CB, Small SA, Petsko GA, Andersen OM (2023)
706 Dimerization of the Alzheimer's disease pathogenic receptor SORLA regulates its

707 association with retromer. Proc Natl Acad Sci U S A 120: e2212180120 Doi
708 10.1073/pnas.2212180120
709 35 Jensen AMG, Raska J., Fojtik P., Monti G., Lunding M., Vochyanova S., Pospisilova V., van
710 der Lee S.J., Van Dongen J., Bossaerts L., Van Broeckhoven C., Dols O., Lleo A., Benussi, L.,
711 Ghidoni R., Hulsman M., Sleegers K., Bohaciakova D., Holstege H., Andersen O.M. (2023)
712 The SORL1 p. Y1816C variant causes impaired endosomal dimerization and autosomal
713 dominant Alzheimer's disease. MedRxiv: Doi 10.1101/2023.07.09.23292253
714 36 Jiao X, Ventruto V, Trese MT, Shastry BS, Hejtmancik JF (2004) Autosomal recessive
715 familial exudative vitreoretinopathy is associated with mutations in LRP5. Am J Hum
716 Genet 75: 878-884 Doi 10.1086/425080
717 37 Josephs KA, Whitwell JL, Tosakulwong N, Weigand SD, Murray ME, Liesinger AM,
718 Petrucelli L, Senjem ML, Ivnik RJ, Parisi JEet al (2015) TAR DNA-binding protein 43 and
719 pathological subtype of Alzheimer's disease impact clinical features. Ann Neurol 78: 697-
720 709 Doi 10.1002/ana.24493
721 38 Katsumata Y, Shade LM, Hohman TJ, Schneider JA, Bennett DA, Farfel JM, Alzheimer's
722 Disease Genetics C, Kukull WA, Fardo DW, Nelson PT (2022) Multiple gene variants linked
723 to Alzheimer's-type clinical dementia via GWAS are also associated with non-Alzheimer's
724 neuropathologic entities. Neurobiol Dis 174: 105880 Doi 10.1016/j.nbd.2022.105880
725 39 Kizhakkedath P, John A, Al-Sawafi BK, Al-Gazali L, Ali BR (2019) Endoplasmic reticulum
726 quality control of LDLR variants associated with familial hypercholesterolemia. FEBS Open
727 Bio 9: 1994-2005 Doi 10.1002/2211-5463.12740
728 40 Knupp A, Mishra S, Martinez R, Braggin JE, Szabo M, Kinoshita C, Hailey DW, Small SA,
729 Jayadev S, Young JE (2020) Depletion of the AD Risk Gene SORL1 Selectively Impairs
730 Neuronal Endosomal Traffic Independent of Amyloidogenic APP Processing. Cell Rep 31:
731 107719 Doi 10.1016/j.celrep.2020.107719
732 41 Kopanos C, Tsiolkas V, Kouris A, Chapple CE, Albarca Aguilera M, Meyer R, Massouras A
733 (2019) VarSome: the human genomic variant search engine. Bioinformatics 35: 1978-
734 1980 Doi 10.1093/bioinformatics/bty897
735 42 Kunkle BW, Grenier-Boley B, Sims R, Bis JC, Damotte V, Naj AC, Boland A, Vronskaya M,
736 van der Lee SJ, Amlie-Wolf Aet al (2019) Genetic meta-analysis of diagnosed Alzheimer's
737 disease identifies new risk loci and implicates Abeta, tau, immunity and lipid processing.
738 Nat Genet 51: 414-430 Doi 10.1038/s41588-019-0358-2
739 43 Lambert JC, Ibrahim-Verbaas CA, Harold D, Naj AC, Sims R, Bellenguez C, Jun G, Destefano
740 AL, Bis JC, Beecham GWet al (2013) Meta-analysis of 74,046 individuals identifies 11 new
741 susceptibility loci for Alzheimer's disease. Nat Genet 45: 1452-1458 Doi 10.1038/ng.2802
742 44 Lee EG, Tulloch J, Chen S, Leong L, Saxton AD, Kraemer B, Darvas M, Keene CD, Shutes-
743 David A, Todd Ket al (2020) Redefining transcriptional regulation of the APOE gene and
744 its association with Alzheimer's disease. PLoS One 15: e0227667 Doi
745 10.1371/journal.pone.0227667
746 45 Leverenz JB, Fishel MA, Peskind ER, Montine TJ, Nochlin D, Steinbart E, Raskind MA,
747 Schellenberg GD, Bird TD, Tsuang D (2006) Lewy body pathology in familial Alzheimer
748 disease: evidence for disease- and mutation-specific pathologic phenotype. Arch Neurol
749 63: 370-376 Doi 10.1001/archneur.63.3.370

750 46 Li H, Durbin R (2009) Fast and accurate short read alignment with Burrows-Wheeler
751 transform. Bioinformatics 25: 1754-1760 Doi 10.1093/bioinformatics/btp324
752 47 Li JK, Li Y, Zhang X, Chen CL, Rao YQ, Fei P, Zhang Q, Zhao P, Li J (2018) Spectrum of Variants
753 in 389 Chinese Probands With Familial Exudative Vitreoretinopathy. Invest Ophthalmol
754 Vis Sci 59: 5368-5381 Doi 10.1167/iovs.17-23541
755 48 Lippa CF, Fujiwara H, Mann DM, Giasson B, Baba M, Schmidt ML, Nee LE, O'Connell B,
756 Pollen DA, St George-Hyslop Pet al (1998) Lewy bodies contain altered alpha-synuclein in
757 brains of many familial Alzheimer's disease patients with mutations in presenilin and
758 amyloid precursor protein genes. Am J Pathol 153: 1365-1370 Doi 10.1016/s0002-
759 9440(10)65722-7
760 49 McKenna A, Hanna M, Banks E, Sivachenko A, Cibulskis K, Kernytsky A, Garimella K,
761 Altshuler D, Gabriel S, Daly M, DePristo MA (2010) The Genome Analysis Toolkit: a
762 MapReduce framework for analyzing next-generation DNA sequencing data. Genome Res
763 20: 1297-1303 Doi 10.1101/gr.107524.110
764 50 Miguel L, Gervais J, Nicolas G, Lecourtois M (2023) SorLA Protective Function Is Restored
765 by Improving SorLA Protein Maturation in a Subset of Alzheimer's Disease-Associated
766 SORL1 Missense Variants. J Alzheimers Dis 94: 1343-1349 Doi 10.3233/JAD-230211
767 51 Mishra S, Knupp A, Szabo MP, Williams CA, Kinoshita C, Hailey DW, Wang Y, Andersen
768 OM, Young JE (2022) The Alzheimer's gene SORL1 is a regulator of endosomal traffic and
769 recycling in human neurons. Cell Mol Life Sci 79: 162 Doi 10.1007/s00018-022-04182-9
770 52 Montine TJ, Phelps CH, Beach TG, Bigio EH, Cairns NJ, Dickson DW, Duyckaerts C, Frosch
771 MP, Masliah E, Mirra SSet al (2012) National Institute on Aging-Alzheimer's Association
772 guidelines for the neuropathologic assessment of Alzheimer's disease: a practical
773 approach. Acta Neuropathol 123: 1-11 Doi 10.1007/s00401-011-0910-3
774 53 Nelson PT, Dickson DW, Trojanowski JQ, Jack CR, Boyle PA, Arfanakis K, Rademakers R,
775 Alafuzoff I, Attems J, Brayne Cet al (2019) Limbic-predominant age-related TDP-43
776 encephalopathy (LATE): consensus working group report. Brain 142: 1503-1527 Doi
777 10.1093/brain/awz099
778 54 Nelson PT, Lee EB, Cykowski MD, Alafuzoff I, Arfanakis K, Attems J, Brayne C, Corrada MM,
779 Dugger BN, Flanagan MEet al (2023) LATE-NC staging in routine neuropathologic
780 diagnosis: an update. Acta Neuropathol 145: 159-173 Doi 10.1007/s00401-022-02524-2
781 55 Pottier C, Hannequin D, Coutant S, Rovelet-Lecrux A, Wallon D, Rousseau S, Legallic S,
782 Paquet C, Bombois S, Pariente Jet al (2012) High frequency of potentially pathogenic
783 SORL1 mutations in autosomal dominant early-onset Alzheimer disease. Mol Psychiatry
784 17: 875-879 Doi 10.1038/mp.2012.15
785 56 Raghavan NS, Brickman AM, Andrews H, Manly JJ, Schupf N, Lantigua R, Wolock CJ,
786 Kamalakaran S, Petrovski S, Tosto Get al (2018) Whole-exome sequencing in 20,197
787 persons for rare variants in Alzheimer's disease. Ann Clin Transl Neurol 5: 832-842 Doi
788 10.1002/acn3.582
789 57 Reitz C (2018) Retromer Dysfunction and Neurodegenerative Disease. Curr Genomics 19:
790 279-288 Doi 10.2174/1389202919666171024122809
791 58 Reitz C, Cheng R, Rogaeva E, Lee JH, Tokuhiro S, Zou F, Bettens K, Sleegers K, Tan EK,
792 Kimura Ret al (2011) Meta-analysis of the association between variants in SORL1 and
793 Alzheimer disease. Arch Neurol 68: 99-106 Doi 10.1001/archneurol.2010.346

59 Rogaeva E, Meng Y, Lee JH, Gu Y, Kawarai T, Zou F, Katayama T, Baldwin CT, Cheng R, Hasegawa Het al (2007) The neuronal sortilin-related receptor SORL1 is genetically associated with Alzheimer disease. Nat Genet 39: 168-177 Doi 10.1038/ng1943

60 Rovelet-Lecrux A, Feuillette S, Miguel L, Schramm C, Pernet S, Quenez O, Segalas-Milazzo I, Guilhaudis L, Rousseau S, Riou Get al (2021) Impaired SorLA maturation and trafficking as a new mechanism for SORL1 missense variants in Alzheimer disease. Acta Neuropathol Commun 9: 196 Doi 10.1186/s40478-021-01294-4

61 Rudenko G, Henry L, Henderson K, Ichtchenko K, Brown MS, Goldstein JL, Deisenhofer J (2002) Structure of the LDL receptor extracellular domain at endosomal pH. Science 298: 2353-2358 Doi 10.1126/science.1078124

62 Scheltens P, De Strooper B, Kivipelto M, Holstege H, Chetelat G, Teunissen CE, Cummings J, van der Flier WM (2021) Alzheimer's disease. Lancet 397: 1577-1590 Doi 10.1016/S0140-6736(20)32205-4

63 Schmidt V, Sporbert A, Rohe M, Reimer T, Rehm A, Andersen OM, Willnow TE (2007) SorLA/LR11 regulates processing of amyloid precursor protein via interaction with adaptors GGA and PACS-1. J Biol Chem 282: 32956-32964 Doi 10.1074/jbc.M705073200

64 Schwenk BM, Hartmann H, Serdaroglu A, Schludi MH, Hornburg D, Meissner F, Orozco D, Colombo A, Tahirovic S, Michaelsen Met al (2016) TDP-43 loss of function inhibits endosomal trafficking and alters trophic signaling in neurons. EMBO J 35: 2350-2370 Doi 10.15252/embj.201694221

65 Simoes S, Guo J, Buitrago L, Qureshi YH, Feng X, Kothiya M, Cortes E, Patel V, Kannan S, Kim YHet al (2021) Alzheimer's vulnerable brain region relies on a distinct retromer core dedicated to endosomal recycling. Cell Rep 37: 110182 Doi 10.1016/j.celrep.2021.110182

66 Small SA, Kent K, Pierce A, Leung C, Kang MS, Okada H, Honig L, Vonsattel JP, Kim TW (2005) Model-guided microarray implicates the retromer complex in Alzheimer's disease. Ann Neurol 58: 909-919 Doi 10.1002/ana.20667

67 Smith JK, Mellick GD, Sykes AM (2022) The role of the endolysosomal pathway in alpha-synuclein pathogenesis in Parkinson's disease. Front Cell Neurosci 16: 1081426 Doi 10.3389/fncel.2022.1081426

68 Sorensen S, Ranheim T, Bakken KS, Leren TP, Kulseth MA (2006) Retention of mutant low density lipoprotein receptor in endoplasmic reticulum (ER) leads to ER stress. J Biol Chem 281: 468-476 Doi 10.1074/jbc.M507071200

69 Thonberg H, Chiang HH, Lilius L, Forsell C, Lindstrom AK, Johansson C, Bjorkstrom J, Thordardottir S, Sleegers K, Van Broeckhoven Cet al (2017) Identification and description of three families with familial Alzheimer disease that segregate variants in the SORL1 gene. Acta Neuropathol Commun 5: 43 Doi 10.1186/s40478-017-0441-9

70 Tosto G, Reitz C (2013) Genome-wide association studies in Alzheimer's disease: a review. Curr Neurol Neurosci Rep 13: 381 Doi 10.1007/s11910-013-0381-0

71 Verheijen J, Van den Bossche T, van der Zee J, Engelborghs S, Sanchez-Valle R, Llado A, Graff C, Thonberg H, Pastor P, Ortega-Cubero Set al (2016) A comprehensive study of the genetic impact of rare variants in SORL1 in European early-onset Alzheimer's disease. Acta Neuropathol 132: 213-224 Doi 10.1007/s00401-016-1566-9

72 Willnow TE, Petersen CM, Nykjaer A (2008) VPS10P-domain receptors - regulators of neuronal viability and function. Nat Rev Neurosci 9: 899-909 Doi nrn2516 [pii]

838 10.1038/nrn2516
839 73 Yamazaki H, Bujo H, Kusunoki J, Seimiya K, Kanaki T, Morisaki N, Schneider WJ, Saito Y
840 (1996) Elements of neural adhesion molecules and a yeast vacuolar protein sorting
841 receptor are present in a novel mammalian low density lipoprotein receptor family
842 member. J Biol Chem 271: 24761-24768 Doi 10.1074/jbc.271.40.24761
843 74 Yamazaki H, Bujo H, Saito Y (1997) A novel member of the LDL receptor gene family with
844 eleven binding repeats is structurally related to neural adhesion molecules and a yeast
845 vacuolar protein sorting receptor. J Atheroscler Thromb 4: 20-26
846 75 Zong Y, Zhang B, Gu S, Lee K, Zhou J, Yao G, Figueiredo D, Perry K, Mei L, Jin R (2012)
847 Structural basis of agrin-LRP4-MuSK signaling. Genes Dev 26: 247-258 Doi
848 10.1101/gad.180885.111
849
850
851
852
853
854

855 # Figure Legends

856

857 **Figure 1. Pedigree of SORL1 R953C family:** Solid black indicates individuals diagnosed with
858 Alzheimer Disease which was confirmed by neuropathology. Dark grey indicates clinical
859 diagnosis of dementia. Onset of disease ("o" years) and age at death "d" years is indicated next to
860 the individual when applicable. Circles indicate female, square indicates male. Diamond is sex
861 unknown to investigators at time of report. + or – indicates presence or absence of *SORL1*
862 c.2857C>T variant. In individuals where APOE genotype was assessed it is indicated on pedigree.
863

864 **Figure 2. Neuropathologic evaluation demonstrates high Alzheimer disease pathologic**
865 **change (ADNC) by NIA-AA criteria in SORL1 R953C cases.** (a) Representative section of
866 cerebellum stained for β-amyloid (6e10), highlighting plaques within the molecular layer and
867 warranting a Thal phase 5. Patient II-5, scale bar = 50 µm. (b) Representative section of calcarine
868 cortex stained for phosphorylated tau (P-Tau; AT8), highlighting neurofibrillary tangles in a
869 background of dystrophic neurites, consistent with Braak and Braak stage VI. Patient II-5, scale
870 bar = 20 µm. (c) Representative section of middle frontal gyrus stained with Bielschowsky silver

871 demonstrating frequent neuritic plaques by CERAD criteria. Insert shows a representative neuritic
872 plaque, composed of brown, targetoid β-amyloid associated with black dystrophic neurites. Patient
873 II-5, scale bars = 50 μm. (d) Representative section of hippocampus stained for phosphorylated
874 TDP-43 (P-TDP43), demonstrating intracytoplasmic inclusions and scattered dystrophic neurites.
875 The pattern is consistent with limbic-predominant age-related TDP-43 encephalopathy (LATE)
876 stage 2, though age < 80 years is atypical for sporadic LATE. Patient II-4, scale bar = 20 μm. (e)
877 Representative section of anterior cingulate gyrus stained for α-synuclein, highlighting the
878 presence of a Lewy body in a background of positive neurites. Though Lewy body disease was
879 present in the majority of SORL1 R953C carriers, the pattern was highly variable. Patient II-2,
880 scale bar = 20 μm.
881
882 **Figure 3. Neuropathology of all family members who consented to autopsy.**
883 Representative photomicrographs demonstrating highest level neuropathologic change in each
884 autopsy case for β-amyloid plaques (6e10 antibody), neurofibrillary tangles (tau antibodies as
885 listed below), neuritic plaques (Bielschowsky silver stain), phosphorylated-TDP-43 inclusions (P-
886 TDP43 antibody), and Lewy bodies (α-Synuclein antibody). (a) Patient I-2, with β-amyloid
887 plaques in the substantia nigra, neurofibrillary tangles (Tau2 antibody) in the calcarine cortex
888 (primary visual cortex), and frequent neuritic plaque density by CERAD criteria (note that silver
889 staining was lighter than other cases). No p-TDP43 or α-synuclein was present, shown here as lack
890 of staining in areas affected early in disease process. (b) Patient II-1, with β-amyloid plaques in
891 the periaqueductal grey matter of the midbrain, neurofibrillary tangles (AT8 antibody) in the
892 calcarine cortex, and frequent neuritic plaque density by CERAD criteria. P-TDP43 inclusions
893 were present in the hippocampus, highlighted by arrows. Lewy bodies were present in brainstem,
894 amygdala, limbic structures, and frontal cortex (shown here). (c) Patient II-2, with β-amyloid
895 plaques in the cerebellum, neurofibrillary tangles in the calcarine cortex (AT8 antibody), and
896 frequent neuritic plaque density by CERAD criteria. P-TDP43 inclusions were present in the
897 hippocampus. Lewy bodies were present in the amygdala and substantia nigra, consistent with a
898 limbic (transitional) pattern. (d) Patient II-3, with β-amyloid plaques in the cerebellum,
899 neurofibrillary tangles in the middle frontal gyrus (AT8 antibody), and frequent neuritic plaque
900 density by CERAD criteria. P-TDP43 inclusions were present in amygdala neurites. No Lewy
901 bodies were observed, demonstrated here by negative staining of the olfactory bulb, one of the

902 earliest anatomic sites of Lewy body formation. (e) Patient II-4, with β-amyloid plaques in the
903 cerebellum, neurofibrillary tangles in the calcarine cortex (Tau2 antibody), and frequent neuritic
904 plaque density by CERAD criteria. P-TDP43 inclusions were present in the hippocampus. Lewy
905 bodies were present in the pigmented cells of the substantia nigra but not in any other site. (f)
906 Patient II-5, with β-amyloid plaques in the cerebellum, neurofibrillary tangles in the calcarine
907 cortex (Tau2 antibody), and frequent neuritic plaque density by CERAD criteria. P-TDP43
908 inclusions were present in the hippocampus. No Lewy bodies were observed, again demonstrated
909 here by negative staining of the olfactory bulb. Scale bars = 20 μm for β-amyloid, p-tau, p-TDP43,
910 and α-Synuclein; scale bars = 50 μm for Bielschowsky silver stain.
911
912 **Figure 4. *In silico* characterization of SORL1 p. R953C**
913 (a) Schematic presentation of the mosaic domain structure of the SORL1 protein comprising from
914 the N-terminal end: VPS10p-domain with accompanying 10CCa/b domains, YWTD-repeated β-
915 propeller domain (with p.R953C location indicated) with accompanying EGF-domain, cluster of
916 11 CR-domains, cluster of 6 3Fn-domains, a transmembrane domain followed by a cytoplasmic
917 tail at the C-terminal end. (b) Three-dimensional model of the SORL1 YWTD-domain folding
918 prepared from coordinates from ModelArchive (Y.Kitago, O.M. Andersen, G.A. Petsko.
919 ModelArchive: https://modelarchiveorg/doi/10.5452/ma-agbg4). (c) Alignment of the ~40 amino
920 acids from each of the six YWTD-repeated sequences corresponding to the blades of the β-
921 propeller with indication of β-strands in grey. The arginine R953 resides at domain position 38 of
922 the sequence located in the loop between strands C and D of the fifth β-blade. Partly conserved
923 domain positions are indicated with bold letters and the consensus residues below the SORL1
924 alignment. Below 5 sequences of YWTD-repeated sequences from homologous receptor proteins
925 with known pathogenic variants corresponding to arginines at position 38. (d) The side chain of
926 Arg-953 from SORL1 provides structural stabilization of the domain folding by an ionic
927 interaction with the side chain of Glu-943 based on the three-dimensional model of the folded
928 YWTD-domain. (e) Close-up of the Arg-Glu pairs from YWTD-domain crystal structures for
929 residues in LDLR, LRP4 and LRP6 (LRP5 homolog) corresponding to pathogenic variants as
930 listed in panel c
931

932 **Figure 5. SORL1 R953C cells are defective in maturation and shedding of the SORL1**
933 **protein.**
934 (a) Representative western blotting of lysate and media samples from HEK293 cells transiently
935 transfected with SORLA-WT or SORLA-R953C. (b) Densitometric analysis from HEK293 and
936 N2a samples. The signal for the R953C is expressed relative to the WT signal. Results are
937 expressed as Mean± SD and analyzed by parametric two-tailed paired t-test. Significance was
938 defined as a value of **p<0. 01, ***p<0. 001. n= 4 independent experiments
939
940 **Figure 6. SORL1 R953C cells have reduced SORL1 protein localization on the cell surface.**
941 (a) Representative immunocytochemistry from HEK293 cells transiently transfected with
942 SORLA-WT or SORLA-R953C expression construct and stained for SORLA (red) at the cell
943 surface. White arrows show positive cells. (b) Flow cytometry dot plot showing surface
944 (AlexaFluor 647 fluorescence) and total (GFP fluorescence) in live single HEK293 cells
945 expressing WT-GFP and R953C-GFP. Vertical and horizontal lines represent thresholds for GFP
946 and AlexaFluor 647-positive cells, respectively. Represented are GFP-positive cells with
947 AlexaFluor 647 signal above (black, inside red dashed gate) or below threshold (dark grey); and
948 untransfected cells (light grey). Numbers in the plots represent the percentages of the cells inside
949 the gates. (c) Bar plots of AlexaFluor 647 fluorescence in HEK293 and N2a cells expressing WT-
950 GFP or R953C-GFP, generated from population of GFP-positive cells. n=3 independent
951 experiments. Results are expressed as Mean± SD and analyzed by parametric two-tailed paired t-
952 test. Significance was defined as a value of ***p<0. 001.
953
954 **Figure 7. SORL1 R953C cells have reduced localization of the SORL1 protein in early and**
955 **recycling endosomes.** HEK293 cells transiently expressing WT or R953C (red) are shown for
956 their colocalization with (a) EEA1 (early endosomal marker), (b) TFR (recycling endosomal
957 marker), and (c) Calnexin (ER marker) (green). The nuclei were visualized with Hoechst (blue).
958 Bar graphs on the right panel illustrate quantifications of colocalization between WT and R953C
959 in cells co-stained for (a) EEA1, (b) TFR and (c) Calnexin. In all cases, the quantification of
960 colocalization was represented as Mander's correlation coefficient. 20-30 images per condition
961 were analyzed. Data are shown as mean±SD and analyzed by parametric two-tailed unpaired t-
962 test. Significance was defined as a value of ****p<0.0001.

963

Figure 1

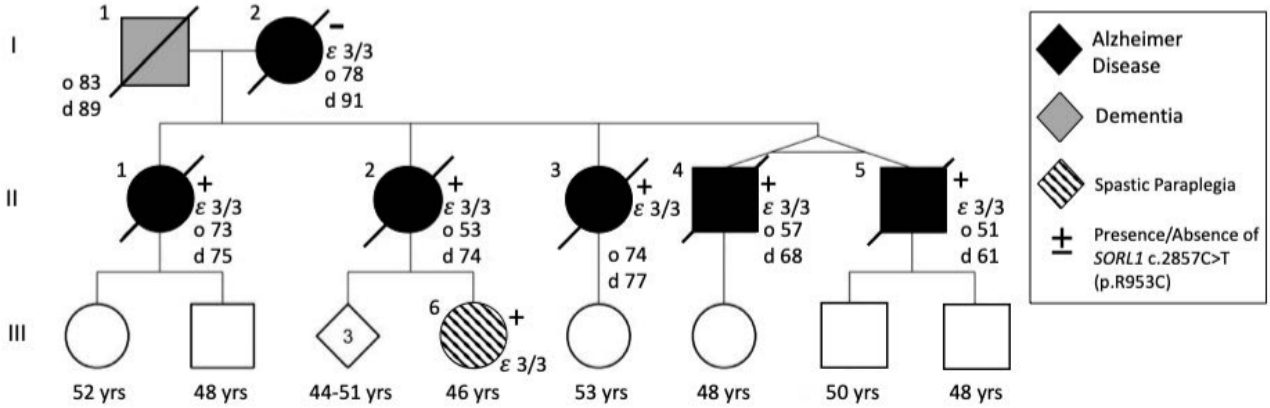
I
II
III
1
o 83
d 89
2
−
ε 3/3
o 78
d 91
1
+
ε 3/3
o 73
d 75
2
+
ε 3/3
o 53
d 74
3
+
ε 3/3
o 74
d 77
4
+
ε 3/3
o 57
d 68
5
+
ε 3/3
o 51
d 61
3
6
+
ε 3/3
52 yrs
48 yrs
44-51 yrs
46 yrs
53 yrs
48 yrs
50 yrs
48 yrs
Alzheimer Disease
Dementia
Spastic Paraplegia
± Presence/Absence of SORL1 c.2857C>T (p.R953C)

Figure 2

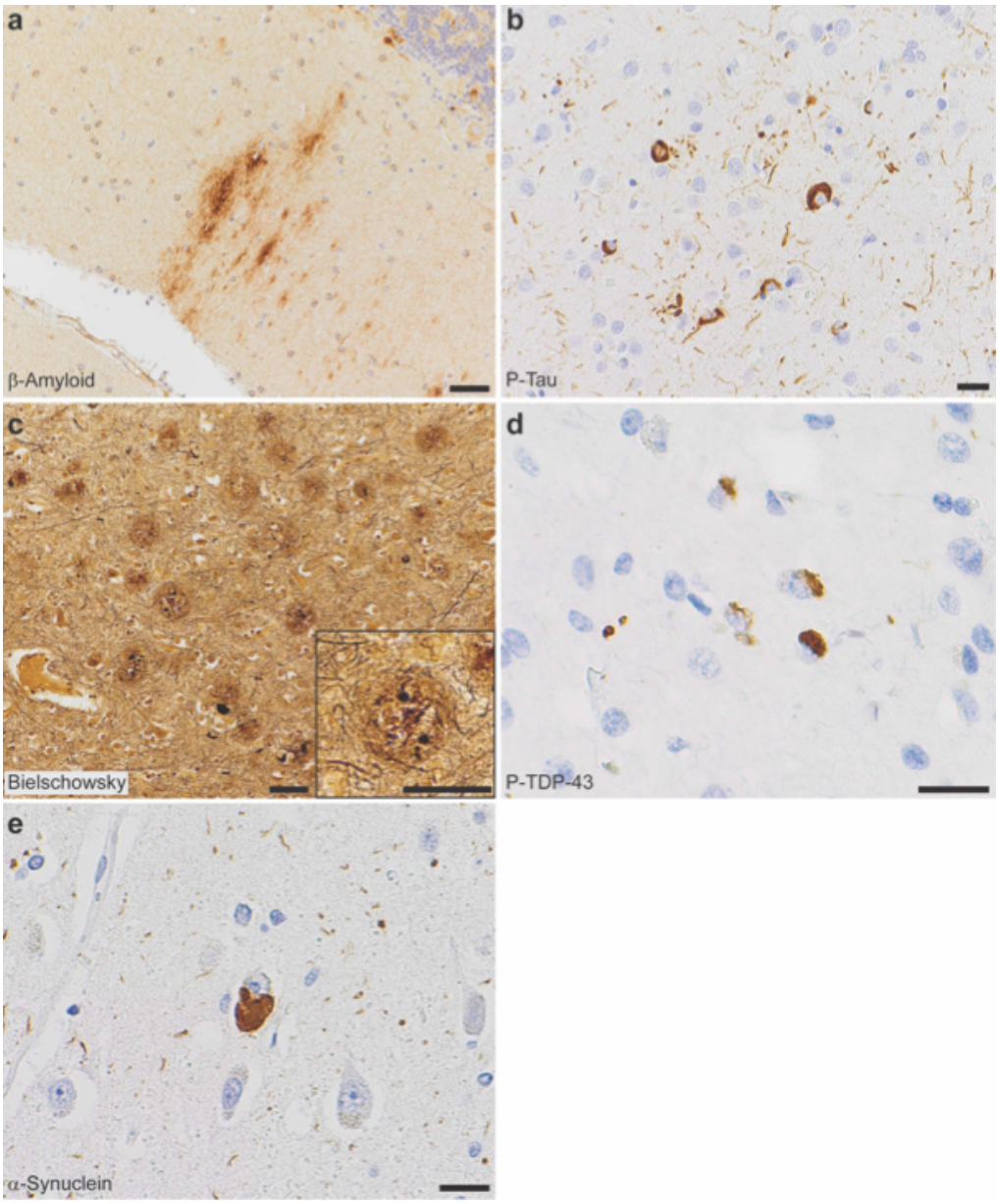

Figure 3

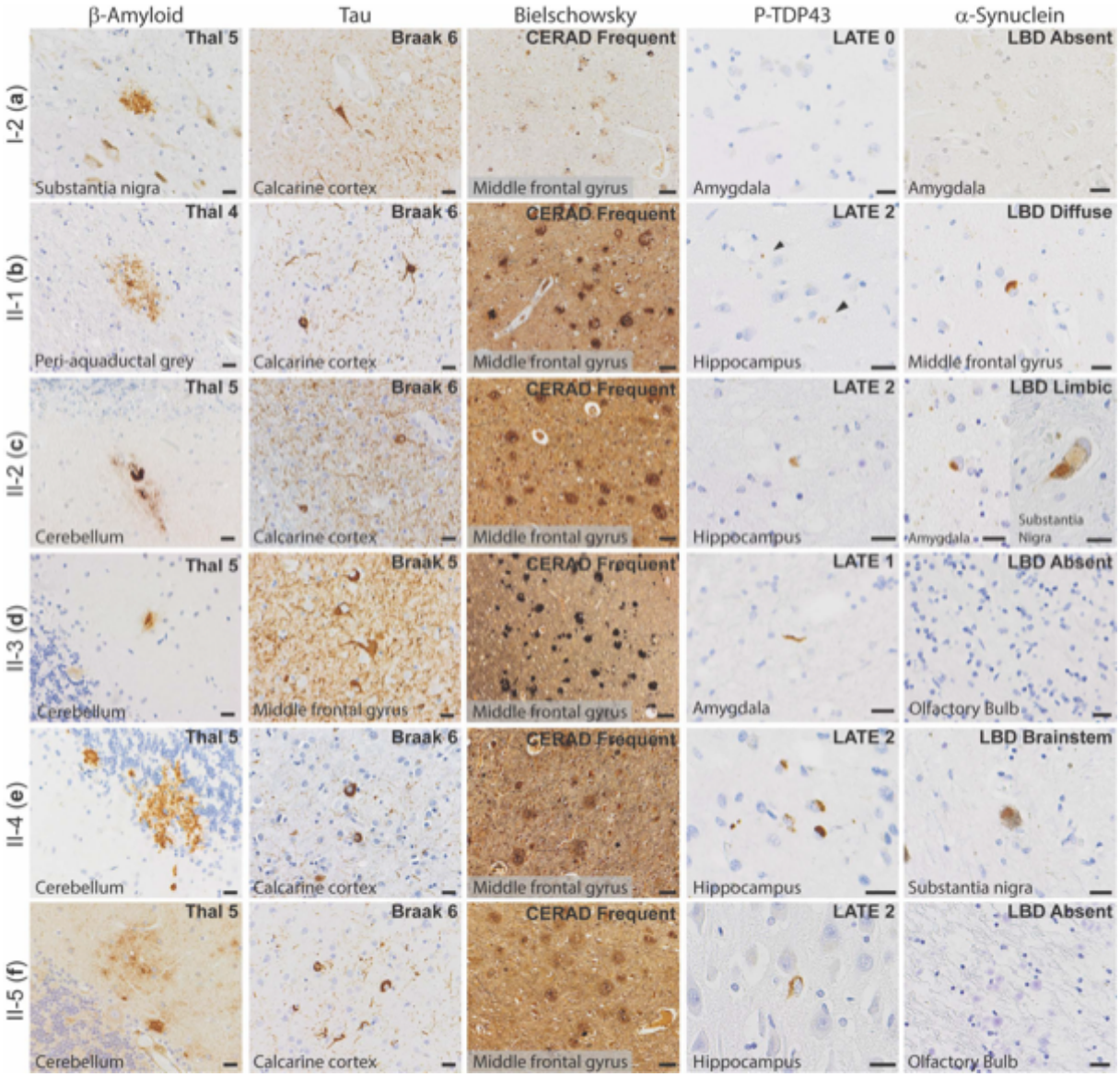
β-Amyloid
Tau
Bielschowsky
P-TDP43
α-Synuclein
I-2 (a)
II-1 (b)
II-2 (c)
II-3 (d)
II-4 (e)
II-5 (f)
Thal 5
Braak 6
CERAD Frequent
LATE 0
LBD Absent
Substantia nigra
Calcarine cortex
Middle frontal gyrus
Amygdala
Amygdala
Thal 4
Braak 6
CERAD Frequent
LATE 2
LBD Diffuse
Peri-aquaductal grey
Calcarine cortex
Middle frontal gyrus
Hippocampus
Middle frontal gyrus
Thal 5
Braak 6
CERAD Frequent
LATE 2
LBD Limbic
Cerebellum
Calcarine cortex
Middle frontal gyrus
Hippocampus
Amygdala
Substantia Nigra
Thal 5
Braak 5
CERAD Frequent
LATE 1
LBD Absent
Cerebellum
Middle frontal gyrus
Middle frontal gyrus
Amygdala
Olfactory Bulb
Thal 5
Braak 6
CERAD Frequent
LATE 2
LBD Brainstem
Cerebellum
Calcarine cortex
Middle frontal gyrus
Hippocampus
Substantia nigra
Thal 5
Braak 6
CERAD Frequent
LATE 2
LBD Absent
Cerebellum
Calcarine cortex
Middle frontal gyrus
Hippocampus
Olfactory Bulb

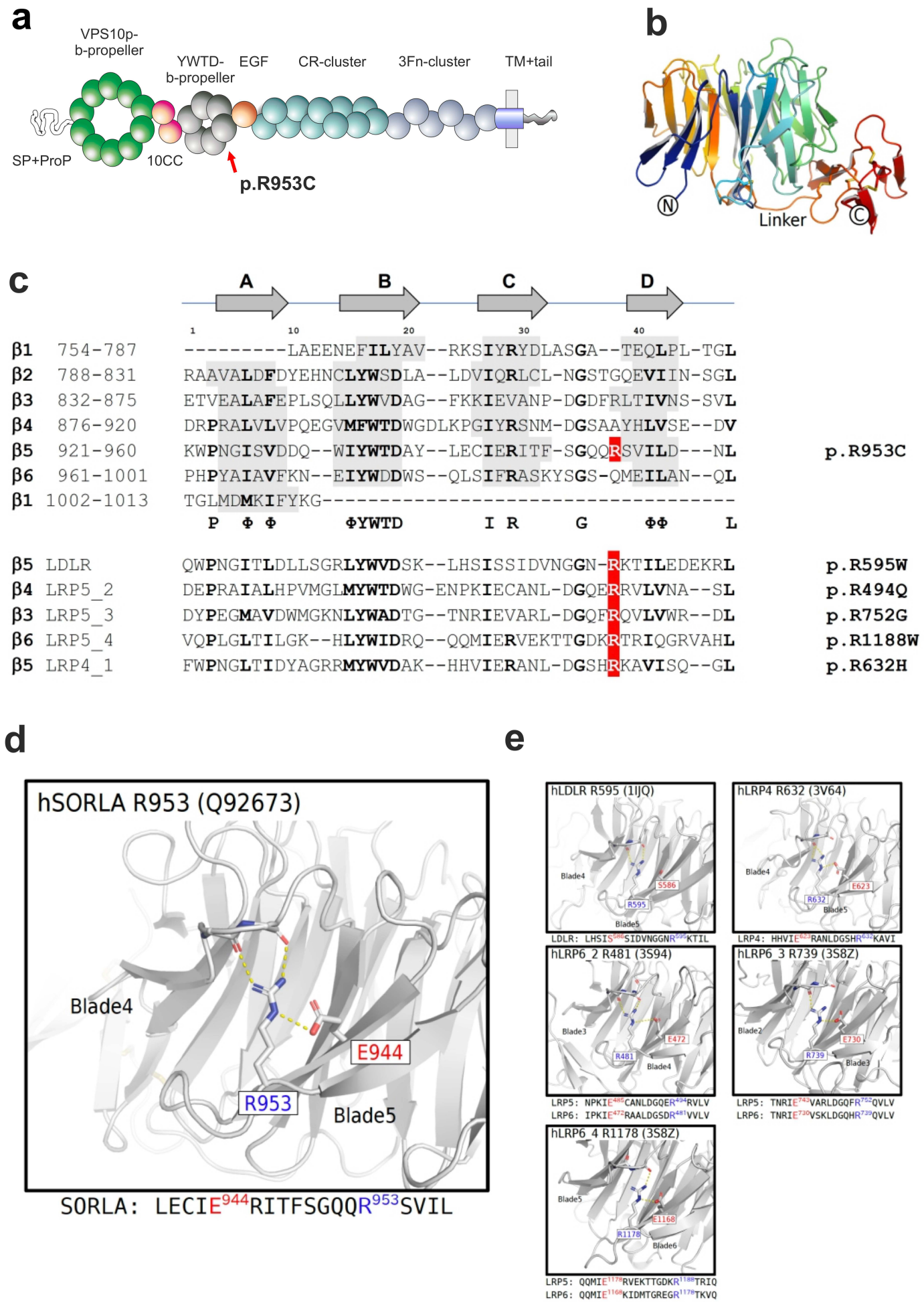
a
VPS10p-
b-propeller
YWTD-
b-propeller
EGF
CR-cluster
3Fn-cluster
TM+tail
SP+ProP
10CC
p.R953C
b
N
Linker
C
c
A
B
C
D
1
10
20
30
40
β1 754-787 ---------LAEENEFILYAV--RKSIYRYDLASGA--TEQLPL-TGL
β2 788-831 RAAVALDFDYEHNCLYWSDLA--LDVIQRLCL-NGSTGQEVIIN-SGL
β3 832-875 ETVEALAFEPLSQLLYWVDAG--FKKIEVANP-DGDFRLTIVNS-SVL
β4 876-920 DRPRALVLVPQEGVMFWTDWGDLKPGIYRSNM-DGSAAYHLVSE--DV
β5 921-960 KWPNGISVDDQ--WIYWTDAY--LECIERITF-SGQQRSVILD---NL p.R953C
β6 961-1001 PHPYAIAVFKN--EIYWDDWS--QLSIFRASKYSGS-QMEILAN--QL
β1 1002-1013 TGLMDMKIFYKG----------
P Φ Φ ΦYWTD I R G ΦΦ L
β5 LDLR QWPNGITLDLLSGRLYWVDSK--LHSISSIDVNGGN-RKTILEDEKRL p.R595W
β4 LRP5_2 DEPRAIALHPVMGLMYWTDWG-ENPKIECANL-DGQERRVLVNA--SL p.R494Q
β3 LRP5_3 DYPEGMAVDWMGKNLYWADTG--TNRIEVARL-DGQFRQVLVWR--DL p.R752G
β6 LRP5_4 VQPLGLTILGK--HLYWIDRQ--QQMIERVEKTTGDKRTRIQGRVAHL p.R1188W
β5 LRP4_1 FWPNGLTIDYAGRRMYWVDAK--HHVIERANL-DGSHRKAVISQ--GL p.R632H
d
hSORLA R953 (Q92673)
Blade4
E944
R953
Blade5
SORLA: LECIE944RITFSGQQR953SVIL
e
hLDLR R595 (1IJQ)
Blade4
S586
R595
Blade5
LDLR: LHSIS586SIDVNGGNR595KTIL
hLRP4 R632 (3V64)
Blade4
E623
R632
Blade5
LRP4: HHVIE623RANLDGSHR632KAVI
hLRP6_2 R481 (3S94)
Blade3
E472
R481
Blade4
LRP5: NPKIE485CANLDGQER494RVLV
LRP6: IPKIE472RAALDGSDR481VVLV
hLRP6_3 R739 (3S8Z)
Blade2
E730
R739
Blade3
LRP5: TNRIE743VARLDGQFR752QVLV
LRP6: TNRIE730VSKLDGQHR739QVLV
hLRP6_4 R1178 (3S8Z)
Blade5
E1168
R1178
Blade6
LRP5: QQMIE1178RVEKTTGDKR1188TRIQ
LRP6: QQMIE1168KIDMTGREGR1178TKVQ

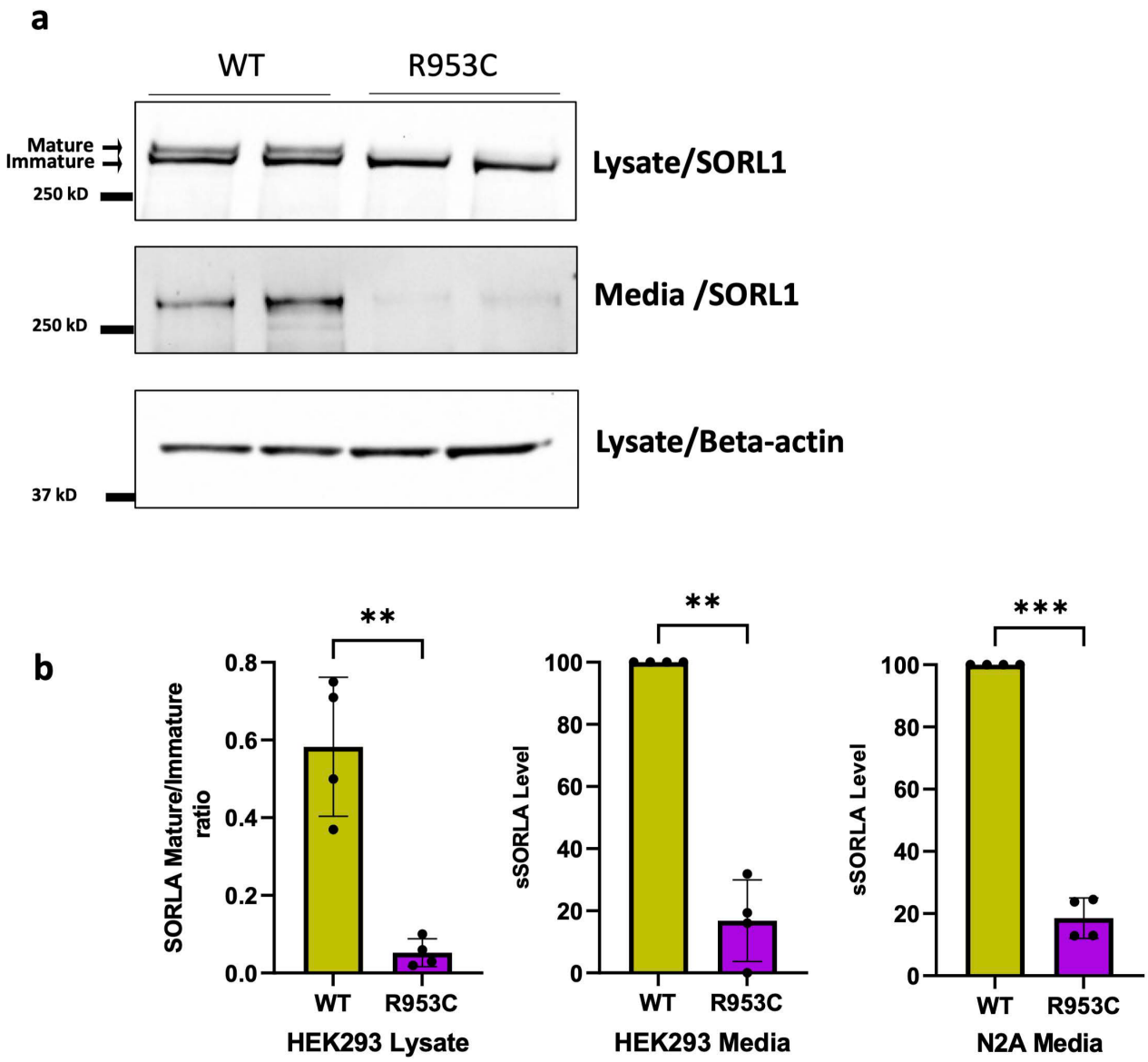
a
WT
R953C
Mature
Immature
250 kD
Lysate/SORL1
250 kD
Media /SORL1
37 kD
Lysate/Beta-actin
b
**
SORLA Mature/Immature ratio
0.8
0.6
0.4
0.2
0.0
WT
R953C
HEK293 Lysate
**
sSORLA Level
100
80
60
40
20
0
WT
R953C
HEK293 Media
***
sSORLA Level
100
80
60
40
20
0
WT
R953C
N2A Media

Figure 6

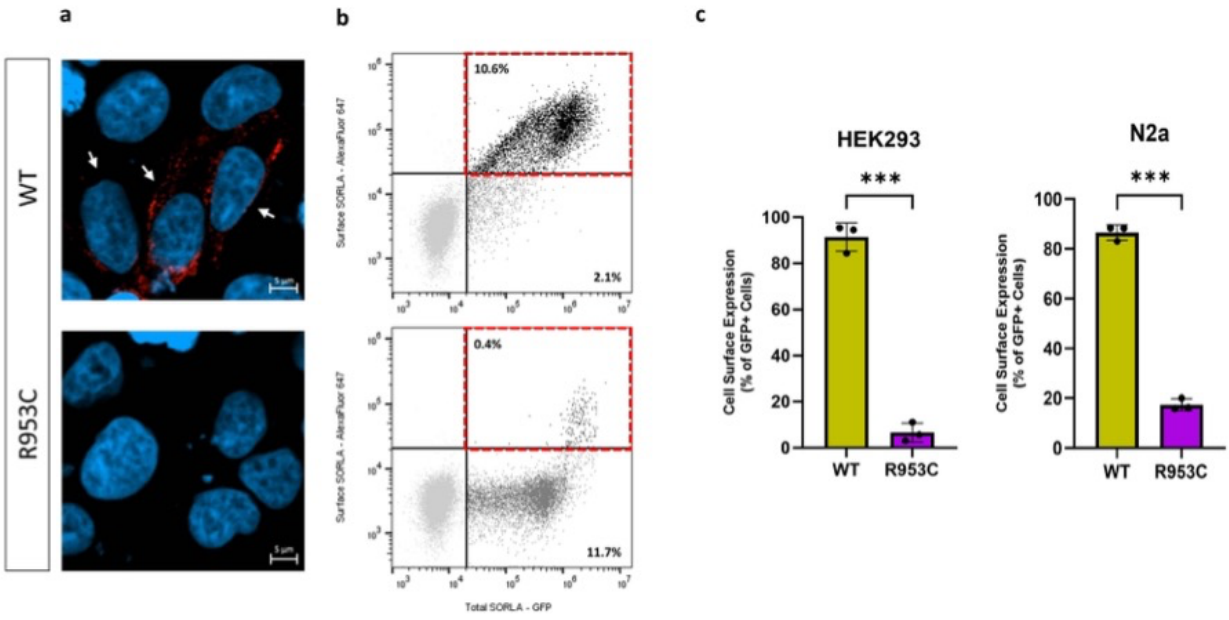
a
WT
R953C
b
10.6%
2.1%
0.4%
11.7%
Surface SORLA - AlexaFluor 647
Total SORLA - GFP
c
HEK293
N2a
***
Cell Surface Expression (% of GFP+ Cells)
WT
R953C

Figure 7

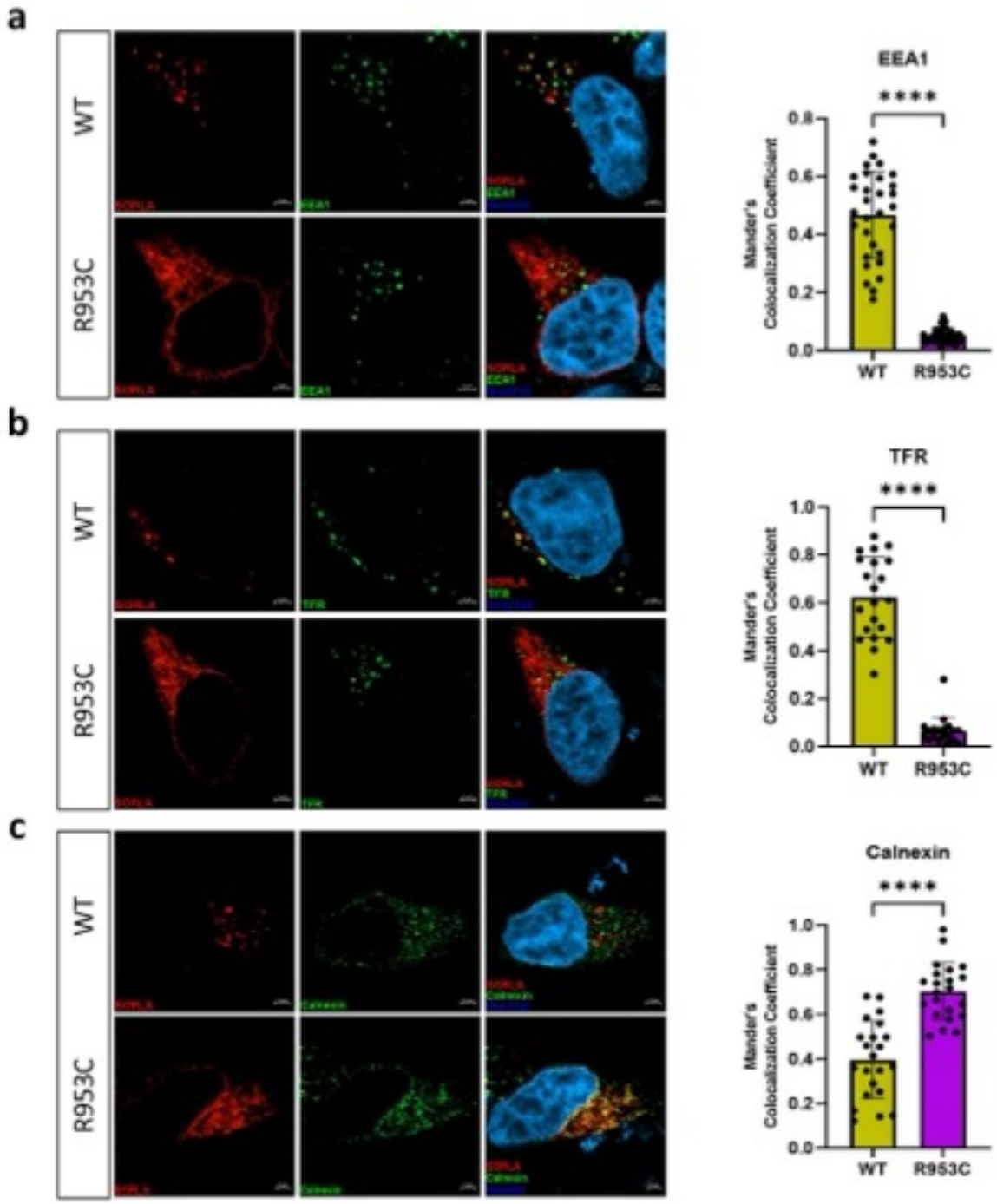
a
WT
R953C
EEA1
****
Mander's Colocalization Coefficient
0.0
0.2
0.4
0.6
0.8
WT
R953C
b
WT
R953C
TFR
****
Mander's Colocalization Coefficient
0.0
0.2
0.4
0.6
0.8
1.0
WT
R953C
c
WT
R953C
Calnexin
****
Mander's Colocalization Coefficient
0.0
0.2
0.4
0.6
0.8
1.0
WT
R953C

Table 1: Clinical Characterization

Clinical Characterization							
ID	**Sex**	**Age of Onset**	**Age at Death**	**Duration (Years)**	**Clinical Features**	**SORL1 genotype**	**APOE genotype**
I-1	M	83	89	6	Dx "Severe Dementia" Parkinsonism Aggressive Behavior	N/A	N/A
I-2	F	78	91	13	Dx Alzheimer Dementia; Age 85 MMSE 23; Age 86 MMSE 15; Age 87 MMSE 11	WT	**3/3**
II-1	F	73	75	2.5	Dx Alzheimer Dementia; Rapid Progression; Age 74 MOCA 11/30	p.R953C	**3/3**
II-2	F	53	74	21	Dx Alzheimer Dementia; Early Memory Loss in 50's; Age 59 WMS "Profound Impairment"; Age 63 MMSE 26	p.R953C	**3/3**
II-3	F	74	77	3	Dx Alzheimer Dementia; Memory loss, aggression, hallucinations, delusions	p. R953C	**3/3**
II-4	M	57	68	11	Dx Alzheimer Dementia; Age 59 MMSE 26; Twin of II-5	p.R953C	**3/3**
II-5	M	51	61	10	Dx Alzheimer Dementia; Aphasia; Apraxia; Age 55 MMSE 9; Twin of II-4	p.R953C	**3/3**
III-6	F	NA	NA	NA	Dx Spastic paraplegia; Age 45 and Age 46; NP testing - executive dysfunction impaired processing and attention	p.R953C	**3/3**

NP =Neuropsychological Testing

Table 2: Neuropathologic Findings

PEDIGREE NUMBER	BRAIN WEIGHT (G)	ATHERO-SCLEROSIS	THAL PHASE	BRAAK STAGE	CERAD	ADNC	HIPPO-CAMPAL SCELROSIS	LATE STAGE	LEWY BODY DISEASE
I-2	900	Moderate	4	VI	Frequent	HIGH	Absent	0	Absent
II-1	1136	Moderate	4	VI	Frequent	HIGH	Absent	2	Diffuse
II-2	867	Moderate	5	VI	Frequent	HIGH	Present	2	Limbic
II-3	1098	Moderate	5	V	Frequent	HIGH	Absent	1	Absent
II-4	950	Severe	II-4	VI	Frequent	HIGH	Present	2	Brain-stem
II-5	1120	Moderate	5	VI	Frequent	HIGH	Absent	2	Absent

Table 3. Homologous mutations for SORL1 R953C in LDLR and LRP

	Disease	SNP	VarSome	Inheritance pattern	References
p.R595W_LDLR	FH	rs373371572	Pathogenic	A.D.	Descamps et al., 2001 Chiou et al., 2010
p.R494Q_LRP5 p.R494W_LRP5	OPPG FEVR	rs121908664 N.A.	Pathogenic Pathogenic	A.R. A.R.	Gong et al., 2001 Ai et al., 2005 Abdel-Hamid et al., 2022
p.R752G_LRP5 p.R752W_LRP5	FEVR OPPG/FEVR	rs121908674 N.A.	Pathogenic Pathogenic	A.R. A.R.	Jiao et al., 2004 Alonso et al., 2015 Hull et al., 2019
p.R1188W_LRP5	PCLD	rs141178995	Pathogenic	A.D.	Cnossen et al., 2014
p.R632H_LRP4	SOST2	N.A.	Likely Pathogenic	A.R.	Huybrechts et a., 2021

N.A. = Not applicable
A.D. =Autosomal Dominant
A.R. =Autosomal Recessive